FINAL REPORT

Predicting DNAPL Source Zone and Plume Response Using Site-Measured Characteristics

SERDP Project ER-1613

MAY 2017

Michael D. Annable
Kirk Hatfield
James W. Jawitz1
University of Florida, Gainesville

Michael C. Brooks
A. Lynn Wood
RS Kerr Research Laboratory US EPA

P. Suresh C. Rao
Purdue University

SERDP
DOD ▪ EPA ▪ DOE

Page Intentionally Left Blank

Page Intentionally Left Blank

REPORT DOCUMENTATION PAGE

1. REPORT DATE (DD-MM-YYYY)	2. REPORT TYPE	3. DATES COVERED (From - To)
5/19/2017	Project Final Report	2007 – 2017

4. TITLE AND SUBTITLE PREDICTING DNAPL SOURCE ZONE AND PLUME RESPONSE USING SITE-MEASURED CHARACTERISTICS

5a. CONTRACT NUMBER
W912HQ-08-C-0049

5c. PROGRAM ELEMENT NUMBER

6. AUTHOR(S) Michael D. Annable, Michael C. Brooks, James W. Jawitz, Kirk Hatfield
P. Suresh C. Rao, A. Lynn Wood

5d. PROJECT NUMBER
ER1613

5e. TASK NUMBER

5f. WORK UNIT NUMBER

7. PERFORMING ORGANIZATION NAME(S) AND ADDRESS(ES)
University of Florida

8. PERFORMING ORGANIZATION REPORT NUMBER

9. SPONSORING / MONITORING AGENCY NAME(S) AND ADDRESS(ES)
SERDP

10. SPONSOR/MONITOR'S ACRONYM(S)

11. SPONSOR/MONITOR'S REPORT NUMBER(S)

12. DISTRIBUTION / AVAILABILITY STATEMENT
Post on SERDP website

13. SUPPLEMENTARY NOTES

14. ABSTRACT This final report and draft guidance document focuses on assessing the level of site characterization needed to support quality decisions regarding remedial strategies and long term stewardship of contaminated sites using a flux and mass balance based approach. Site characterization efforts are aimed at understanding the link between dense nonaqueous phase liquid (DNAPL) source zones mass discharge under natural hydrological conditions and modified as a result of source zone treatment. The transition between forward and back-diffusion was also explored. Specific objectives of this project were to: 1) Develop source-strength functions for site management purposes using existing historical site data supplemented with limited flux- and core-based sampling; 2) Extend to the field-scale our ability to predict DNAPL source depletion through dissolution, based on a priori characterization of the source zone architecture; 3) Characterize the near-source plume response to source-mass depletion at selected field sites in order to provide the understanding needed to predict long-term plume responses; 4) Link the characterization of the near-source, short-term responses to likely long-term behavior of the dissolved plume including back diffusion; and 5) Provide recommended guidance on the level of source zone characterization needed to adequately predict source-strength functions and plume response.

15. SUBJECT TERMS DNAPL Source Strength Function, contaminated sites

16. SECURITY CLASSIFICATION OF:			17. LIMITATION OF ABSTRACT	18. NUMBER OF PAGES	19a. NAME OF RESPONSIBLE PERSON Michael D. Annable
a. REPORT	b. ABSTRACT	c. THIS PAGE		69	19b. TELEPHONE NUMBER (include area code)

Page Intentionally Left Blank

Abstract

This final report and draft guidance document focuses on assessing the level of site characterization needed to support quality decisions regarding remedial strategies and long term stewardship of contaminated sites using a flux and mass balance based approach. Site characterization efforts are aimed at understanding the link between dense nonaqueous phase liquid (DNAPL) source zones mass discharge under natural hydrological conditions and modified as a result of source zone treatment. The transition between forward and back-diffusion was also explored. This document provides an overview of methodologies that can be used to characterize source zone mass discharge functions and how this controls plume response and back diffusion.

Prediction of the relationship between DNAPL source zone changes and down-gradient plume response is critical to making informed site management decisions, especially those related to remedial actions. Thus, it is vital that source zone and plume characterization be conducted within a framework that is consistent with appropriate predictive models. The project focused on demonstration of effective field-scale approaches that provide vital links between characterization, prediction, and decision making.

Specific objectives of this project were to: 1) Develop source-strength functions for site management purposes using existing historical site data supplemented with limited flux- and core-based sampling; 2) Extend to the field-scale our ability to predict DNAPL source depletion through dissolution, based on a priori characterization of the source zone architecture; 3) Characterize the near-source plume response to source-mass depletion at selected field sites in order to provide the understanding needed to predict long-term plume responses; 4) Link the characterization of the near-source, short-term responses to likely long-term behavior of the dissolved plume including back diffusion; and 5) Provide recommended guidance on the level of source zone characterization needed to adequately predict source-strength functions and plume response.

The research effort developed source-strength functions, $M_D(t)$, using existing historical data at field sites. We selected five primary field sites and up to ten secondary sites with available sets of high quality historical data. At the primary sites, additional data was collected. Characterization of the source-strength function were based on a quality historical record of concentration and head measurements, particularly in the near-source region. For each site considered, currently available data alone was used to provide the best possible description of the source function. Following completion of this exercise on secondary sites, primary sites were selected. Sites were evaluated to identify what type of additional data will be obtained including flux-based measurements such as integral pump tests and passive flux meter (PFM) well screen

profiles. The data collected from the primary sites was used to improve the estimated source-strength function and associated error estimates.

Advanced characterization of the DNAPL architecture included current source zone mass (M_0), contaminant fluxes, $J(x,y,z)$, and mass discharge rate, M_D; high-resolution DNAPL saturation characterization, $S_N(x,y,z)$; and trajectory-integrated DNAPL saturation. Mass flux measurements made at down-gradient control planes, and tracer-based trajectory-integrated data are Lagrangian characteristics that contain information representing the actual flow paths taken by water traversing the source zone. Point-based spatial data such as soil cores contain different information, and both data types will be used here to predict dissolution.

At the Alameda California primary site selected for further evaluation, the down-gradient response to changing source zone strength was quantified through a controlled field experiment. The experiment was conducted by containing a portion of an existing source zone using three injection wells and four extraction wells forming a hydraulic control cell. Within this flow cell, the source-strength function behavior under enhanced groundwater flow conditions was observed. Reactive and nonreactive tracers were used to characterize transport conditions within the flow cell including diffusion into lower conductivity zones with the aquifer. The subsequent response of the contaminant plume to a source-strength function perturbation was monitored for "back diffusion" from lower conductivity zones or DNAPL contaminated zones.

The field data collected in this project was used to evaluate several approaches for estimating the source strength function, and the uncertainties associated with the estimated model parameters. Cost-effective approaches to DNAPL site characterization allows Department of Defense (DoD) users and site managers to more accurately assess the benefits of costly aggressive source zone treatment technologies. Accurate assessment of near-source flux changes and the magnitude of "back diffusion" expected will help DoD by avoiding costly remedial efforts with inadequate benefits.

The results of the project can be used by DoD site managers and consultants to better characterize sites in order to make informed decisions regarding implementing aggressive source zone remedial efforts. Guidelines on site characterization efforts aimed at understanding the link between the site DNAPL source strength function under natural hydrological conditions and as modified by source treatment. These guidelines provide an established methodology for defining the source strength function and how this function defines predicted plume responses. The ability to better characterize these relationships can reduce site management and clean-up costs by enabling quantitative prediction of the benefits of costly source zone treatment. In addition, this project developed and disseminated, through journal articles, recommended guidelines and workshops, an approach for quantifying "back diffusion" processes at contaminated sites.

Table of Contents

1. Objectives

Specific objectives of this project were to: 1) Develop source-strength functions for site management purposes using existing historical site data supplemented with limited flux- and core-based sampling; 2) Extend to the field-scale our ability to predict DNAPL source depletion through dissolution, based on a priori characterization of the source zone architecture; 3) Characterize the near-source plume response to source-mass depletion at selected field sites and within an isolated section of the aquifer, to provide the understanding needed to predict long-term plume responses including back diffusion; 4) Link the characterization of the near-source, short-term responses to likely long-term behavior of the dissolved plume; and 5) Provide recommended guidance on the level of source zone characterization needed to adequately predict source-strength functions and plume response.

2. Background

a. Development of Mass Flux Based Evaluation of DNAPL Contaminated Sites

The characterization of DNAPL contaminated sites is shifting the focus to techniques that can lead to a flux based assessment of both contaminants and groundwater, rather than focusing primarily on concentration measurements. Flux data provides the ability to integrate information leading to mass discharge, source mass balances, and changes in mass balance over time. The primary challenge with DNAPL sites is generated by the density contrast between the immiscible phase and water. DNAPL will migrate below the water table, and become trapped on media interfaces. The migration of DNAPL results in varying distributions within the subsurface, and challenges our ability to implement remedial methods.

Site characterization must begin with site assessment, addressing the type of contaminants, the concentration of contaminants in water samples, and the spatial extent of the contaminated area. For each contaminant there is a regulatory maximum contaminant level (MCL). If a NAPL is suspected, the concentrations may be compared to the solubility limit of the NAPL mixture present in the aquifer. The extent of the source zone is then determined, and the site is divided into a source zone and a plume. Remedial technologies are assessed for either source zone or plume, depending on the further characterization of the zones. Remediation is then optimized for cost effectiveness and time effectiveness.

The source zone and the plume are divided distinctly within a model; however there may be secondary source zones as well as back-diffusion of mass that may extend the plume.
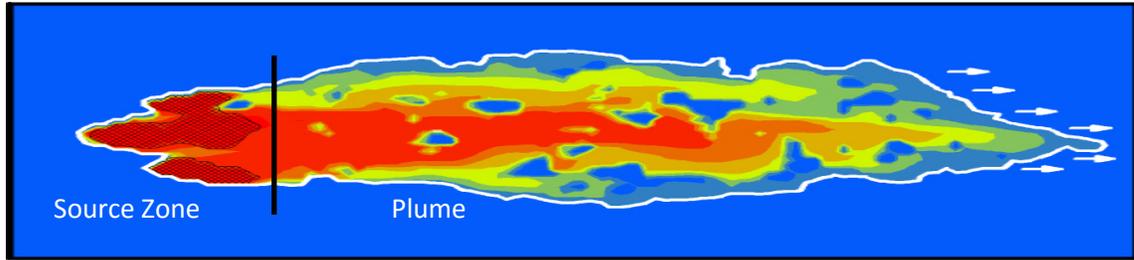
Figure 1.1 Conceptual site with source zone and plume.

Contaminant mass flux and integrated mass discharge have been defined and characterized for sites. Contaminant mass flux has units of mass/area/time, and is the mass of contaminant moving across a unit area of porous media perpendicular to groundwater flow. Integrated mass flux is the total mass moving across an area, over time. A control plane may be defined as the cross section the total contaminant mass is crossing, and generally covers the entire plume. The units of measurement for integrated mass flux are mass/time. Characterizing mass flux and mass discharge becomes useful while investigating attenuation processes, whether natural or enhanced, remedial assessments, measuring loads to receiving bodies, and risk assessment.

Spatial and temporal methods of measurement can be used to quantify mass flux and integrated mass discharge. Point-scale techniques use multilevel samplers and passive flux meters within screened wells, and both methods help to define mass flux. The mass flux data can then be integrated to obtain mass discharge. Integral pump tests can also be implemented for large volumes of water being pumped from the aquifer from fully screened wells. Integral pump tests lack spatial scales of measurement, but offer a "plume core." Each method is investigated to determine the usefulness for site characterization.

Flux measurements have been developed in order to better assess contaminated DNAPL sites. The primary advancement has focused on the relationship between the contaminant mass present in the NAPL source zone, and the contaminant mass flux (source strength) which forms the plume. Site management strategies are now using the fundamental knowledge based on mass flux, mass discharge, and mass balance. Site age, defined as the relative mass remaining in the source area compared to the original mass estimate, allows information regarding site characterizations. Site age considerations and plume longevity may also provide insight for site assessments.

DNAPL sites include difficulties and uncertainties pertaining to site assessment. In order to better characterize DNAPL sites, advancements for better, faster, and cheaper methods for contaminant spatial distribution and integrated spatial or temporal measurements have been the primary focus. The first method offers a more detailed set of measurements, but becomes costly. The second method may lack the spatial or temporal resolution necessary. Cost constraints and the necessity of quantity of data determine which method to use, resulting in a tradeoff from the cost effectiveness and the amount of data being utilized.

The quantity and quality of subsurface site data compared with site hydrogeology and geochemistry control site management decisions along with risk assessment, regulatory requirements, and long term goals.

Prior to mass flux and mass discharge, concentration measurements have been the focus of contaminant regulations. The relationship between mass flux and plume response is the key component to changing the focus from target level concentrations. This quantitative relationship provides a better understanding of the site and allows for more sound decision making. This also allows for a better understanding of the flux distribution from source zones, which may be more cost effective for remedial designs by focusing on the zones that provide the most significant load to the plume, rather than the areas with the highest concentration, which may not be contributing significantly to the plume. Prioritizing limited resources may also be necessary for sites where mass cannot be removed completely, and targeting regions responsible for plume behavior must be the focus.

The ITRC DNAPL team identified six areas where mass flux and/or mass discharge can improve site management (ITRC, 2010):

- Site conceptual model and site characterization
- Threat and exposure evaluation
- Remediation selection and design
- Performance monitoring and optimization
- Compliance and long-term monitoring
- Site prioritization

There may be sites with multiple improvements, but the most vital is the understanding of the site.

Understanding DNAPL sites by the collection of contaminant flux data allows the improvement of site management and decisions. Flux data improves the ability of risk assessment and implementation of remedial actions. Traditional site data collection and historical site data can estimate contaminant mass in source zones and plumes, and can provide a better understanding for source vs. plume remediation.

b. Mass Discharge and Mass Flux as Measures in Site Characterization and Management

Mass flux and mass discharge describe the transport of heat, mass, or volumes of contaminant from the source to the plume. A system mass balance includes those terms, and defines the system conditions. Mass flux, J [M/L^2/T], is defined as the product of the Darcy flux, q[L/T], and the local concentration of contaminant, C [M/L^3], in the aqueous phase

$$J = q\mathrm{C} \quad .\tag{Eq. 1}$$

The Darcy flux can be calculated applying Darcy's Law along the direction of the plume axis at the location of interest:

$$q = -K\frac{dh}{dx} \quad ,\tag{Eq. 2}$$

K is the hydraulic conductivity [L/T], and h is the head measurement at the point of interest. The x direction is selected as the maximum gradient direction. Darcy flux and mass flux are vector quantities, and thus require a direction. Typically the average flux vectors are associated with the flux direction. Although groundwater flow is dynamic, and contaminant mass flux changes direction, the focus is on a large frame scale, resulting in an average Darcy flux direction.

The contaminant mass flux is calculated across a control plane, or a transect, which is perpendicular to the plume axis. Integrating the mass flux with the transect as the spatial extent, quantifies mass discharge, and results in a scalar quantity. A positive value represents the transport in the plume growth direction.

$$M_D = \int_A J dA\tag{Eq. 3}$$

Mass discharge may vary with position and time. Source zone mass discharge is that of the down-gradient edge of the source zone, and how it changes with natural dissolution results in the source strength function, $M_D(0,t)$. The relationship between the source zone and the plume can be used to estimate source/plume mass balance which in turn can be used to assess site conditions.

Site age is again defined as the fraction of the initial source zone mass that has been removed from the source zone through dissolution, volatilization, or degradation, and may contribute to site evaluation. The solubility limit of the contaminant, the groundwater flow velocity, the size of the source zone within the flow direction, and the average NAPL saturation along the flow path may affect the site age.

The average of the mass flux over sections of a cross-section may be useful for large scale evaluations. The integral pump test utilizes multiple wells within a transect. The average mass flux over an area B can represent a potential impacted well from a capture zone of the same area.

$$\bar{J} = \frac{\int_B J dB}{B}\tag{Eq. 4}$$

4

Average concentrations based on flux can be calculated as C = J/q which relates flux to concentration, which may be useful for target concentrations.

Contaminant distribution among phases and projection of mass discharge history are vital for site management. Source depletion occurs with an increasing of mass discharge, and future projections depend on mass discharge dynamics. Declining mass discharge suggests that the majority of the mass is depleted from the source zone, and is now within the plume.

Although mass discharge rates are dynamic and attenuation rates also vary, hydrodynamic characteristics of the aquifer and biogeochemical conditions also contribute to the dissolved plume characteristics. Steady-state (no growth) conditions occur when the contaminant mass discharge from the source zone is equal to the overall mass attenuation rate within the plume. If the attenuation is greater than the mass discharge, then the plume is expected to shrink, but if the attenuation rate is less than the mass discharge, then the plume is expected to grow.

Mass discharge history may be obtained from measurements of the source zone and plume. This history provides knowledge about the site and offers possible projections of mass discharge of the DNAPL.

3. Methods for Evaluating DNAPL Source Dissolution

a. Relationship between Mass Depletion, Mass Discharge and Mass Flux

Source treatment and its impact on mass discharge has been examined with modeling analysis, specifically the REMCHLOR model. Due to hydrogeological conditions and DNAPL distributions, a variety of changes may result. After removal of source mass, contaminant mass discharge reduces significantly according isolated testing cells. Actual field measurements may have alternate results.

i. Power Law Model

The power law source depletion model (PLM) in coordination with the REMCHLOR model, relates the flux-averaged concentration to the source mass empirically. Γ is a function of both media and DNAPL variability.

$$\frac{C_f(T)}{f_c C_s} = \left[\frac{M(T)}{M_0} \right]^{\Gamma} \tag{Eq. 5}$$

where $M(T)$ is the mass remaining in the source zone [M] and M_0 is the initial source mass [M]. Falta et al (2005a) derived an analytical solution for dissolution under the PLM,

$$\frac{C_f(T)}{f_c C_s} = \frac{1}{M_0^\Gamma} \left[\frac{(\Gamma-1)M_{D,0}}{M_0^\Gamma} t + M_0^{1-\Gamma} \right]^{\frac{\Gamma}{1-\Gamma}} \qquad \text{(Eq. 6)}$$

where $M_{D,0}$ is the initial mass discharge (M/T).

ii.   Streamtube Model

The equilibrium streamtube model (ESM) is an analytical model proposed to simulate DNAPL dissolution, and is based upon a Lagrangian approach.

$$\frac{C_f(T)}{f_c C_s} = \frac{1}{2} - \frac{1}{2} erf\left(\frac{\ln T - \mu_{\ln\tau}}{\sigma_{\ln\tau}\sqrt{2}} \right) \qquad . \qquad \text{(Eq. 7)}$$

Here C_f [ML^{-3}] is the flux-averaged concentration existing the source zone; T is the number of pore volumes of natural flowing groundwater that have moved through the source zone [-]; f_c is the fraction of the streamtubes initially containing DNAPL [-], C_s is the solubility limit [ML^{-3}]; τ is defined as reactive travel time that combines the travel time (t) and the trajectory-averaged DNAPL content $\hat{S}$ ($\hat{S} = \dfrac{\hat{S}_N \eta}{\theta_w}$), where $\hat{S}_N$ is the trajectory-averaged DNAPL saturation along a streamline [L^{3}L^{-3}], η is the porosity [L^{3}L^{-3}], and θ_w is the water content [L^{3}L^{-3}]; $\mu_{\ln\tau}$ and $\sigma_{\ln\tau}$ are the mean and standard deviation of the log normal variable $\ln\tau$. The travel time and the DNAPL content $\hat{S}$ are both assumed to be lognormal variables, so the reactive travel time obeys the lognormal distribution.

iii.   Mass Transfer Model

Parker and Park (2004) presented a simplified model for estimating DNAPL source zone mass depletion using an effective Damkohler number, Da:

$$\frac{C_f(T)}{C_s} = 1 - \exp[-Da] \qquad \text{(Eq. 8)}$$

Here, $Da = k_{eff} L_s / \overline{q}$ where k_{eff} [T^{-1}] is the field-scale effective mass transfer coefficient, L_s is the source zone length in the mean flow direction [L], and $\overline{q}$ [LT^{-1}] is the average Darcy flux for the source zone. The effective mass transfer coefficient (k_{eff}) is related to changes in the DNAPL mass and the average groundwater velocity (Parker and Park, 2004).
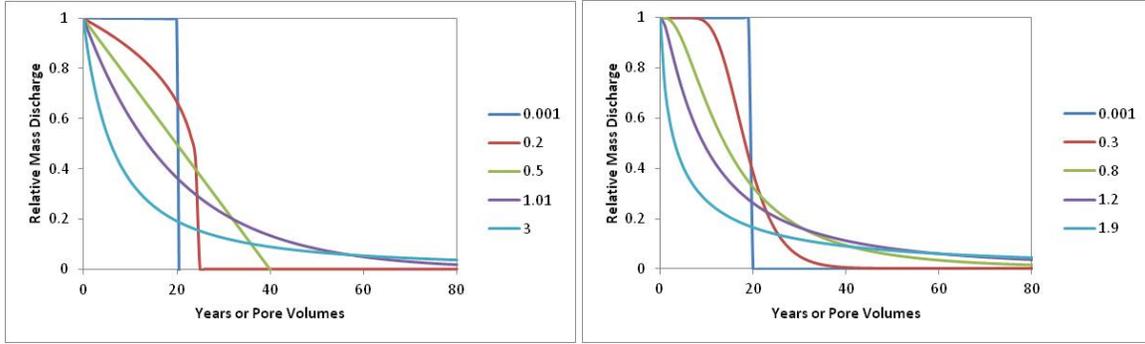
Figure 2.1. Power law (PLM) and Equilibrium Streamtube (ESM) models for source zone dissolution.

a. Site Mass Balance Considerations

i. Plume, Source and Diffusion Domain Mass Distribution

Mass from the plume is linked with mass from the source zone through the historical source strength function. Mass flux and mass discharge relate to site wide mass balance, which can be useful when using estimates for the site.

ii. Concept of Site Age and Aging

Source mass estimation can be estimated using an exponential source decay model using data from wells located near the source.

$$M_{t2} = M_{t1} \exp(-(t_2 - t_1)k) = \frac{qAC_{t1}}{k} \exp(-(t_2 - t_1)k) \qquad \text{(Eq. 9)}$$

where M_{t1} and M_{t2} are the source masses [M] at two different times, and C_{t1} is the concentration [ML^{-3}] in the monitoring well at time t_1 [T]. Using equation 7.9, the present DNAPL source mass (M_{t2}) can be estimated.

Another exponential source decay model assumes zero degradation rates in the plume, a measure of source strength at some time t_2, and an estimated plume mass at that time.

$$M_{P,t2} = \int_0^{t2} M_{D,0} \exp\left(\frac{M_{D,0}}{M_0} t\right) dt = M_0 \left(1 - \exp\left(\frac{M_{D,0}}{M_0}\right) t_{t2}\right) \qquad \text{(Eq. 10)}$$

$$M_{D,t2} = M_{D,0} \exp\left(\frac{M_{D,0}}{M_0} t_{t2}\right) \qquad \text{(Eq. 11)}$$

There are five methods discussed that approximate source strength functions at field sites, and they include spatial and temporal concentration data.

iii. Mass Discharge and Flux during Plume Evolution

Using an advection-dispersion model along with a source strength function provides the ability to implement site characterization from field data that was collected from years of investigation.

Wells located closer to the source zone better represent source zone behavior due to influence on contaminant concentration in areas further from the source zone. A maximum spatial distance may be used to better reflect source zone behavior, but only if there are a sufficient number of measurements.

4. Estimating Source Strength Functions at Field Sites

Mass discharge can vary significantly between sites, and mass flux can also vary within the same site. Quantifying source strength functions is discussed in the next sections.

a. Use of Time Series Data

i. Considering Entire Plume Water Quality Data

One method of fitting an unknown source strength function to the concentration time series field data is to fit the data globally, and try to optimize the parameters Γ or $\sigma_{ln\tau}$. With this method there is likely a distribution of parameters that must be used to represent plume response, most often at higher aged sites or sites with a large contaminant plume.

ii. Individual Well Water Quality Data Series

Contrary to global optimization, the data from individual wells can used to fit source strength function parameters. The distribution of parameter values can be used to estimate a range of values; however the uncertainty is higher due to outliers from other processes occurring within the plume. Optimization for each well for a limited number of parameters can be more effective and less computationally intensive.

b. Use of Transects

Wells must be placed perpendicular to the flow field down-gradient of the source zone when using transects. Transects allow mass discharge data to be collected temporally or spatially, and contains minimal effects of noise in concentration data. Mass discharge across transects can be calculated using a number of methods, but in general it can be summarized as

$$M_D = \sum_{i=1}^{n} q_i C_i A_i \qquad . \qquad \text{(Eq. 12)}$$

Mass fluxes can be measured using passive flux meters, multilevel samplers, stochastic methods, or a combination of these. Mass discharge can be calculated by interpolation from mass flux data. A rigorous stochastic analysis may improve accuracy.

i. Temporal Transects

Observing the change in flux values in time results in a mass discharge time series, which can then be fit to source strength functions. One assumption being made is that the transect is close enough to the source zone to reduce error.

ii. Spatial Transects

Transect data collected in space uses multiple well transects spaced down the plume centerline. This allows for a translation of concentrations from space to time, and is done using travel time using assumed retardation and groundwater velocity between transects. Losses must be considered such as complete degradation, changes in hydro-stratigraphy, and remediation.

c. Use of Extraction Wells

Changes in concentrations in time in extracted contaminated groundwater can be analyzed for changes in source strength, which can predict efficiencies and source behavior from remediation. Although it's possible to fit a source strength function to the cumulative mass removal, natural groundwater gradients may not be reflected by the source strength function of this pumping. The exponential decay model is a simple model that data can be fit to represent source strength function characteristics.

$$\frac{M_A}{M_{A,0}} = \frac{J}{J_0} = \frac{Cq}{J_0} \qquad \text{(Eq. 13)}$$

Here M_A is the mass of contaminant per unit area perpendicular to the groundwater Darcy flux q, J is the mass flux, C is contaminant concentration and the 0 subscripts denote initial values. Thus writing an equation for mass loss:

$$\frac{dM_A}{dt} = -Cq \qquad \text{(Eq. 14)}$$

The solution for the exponential decay model can be written:

$$C = C_0 \exp\left(-\frac{J_0}{M_{A,0}}t\right) \qquad \text{(Eq. 15)}$$

This function can be easily fit to a concentration time series data to determine the unknown values C_0 and ($J_0/ M_{A,0}$).

The more general Power source function model can also be applied to *C(t)* data. The solution used to fit to *C(t)* data employs the following relationship between source zone mass and mass flux:

$$\frac{J}{J_0} = \left(\frac{M_A}{M_{A,0}}\right)^{\Gamma}$$

(Eq. 16)

This can be solved, yielding

$$C = C_0 \left[1 + \frac{J_0(\Gamma - 1)}{M_{A,0}}t\right]^{\frac{\Gamma}{1-\Gamma}}$$

(Eq. 17)

This function with three fitting parameters C_0, Γ and $J_0/M_{A,0}$ can also be fit to the field data sets.

5. Methods for mass discharge and mass flux measurement

Spatial and temporal scales of measurement are two methods that quantify local contaminant flux and integrated mass discharge. Mass flux can be calculated from point scale techniques within screened wells, and that data can be spatially integrated to determine mass discharge. Integral pump tests collect data over fully screened wells and large volumes of water pumped from aquifers, and although it lacks spatial resolution, "plume cores" are incorporated.
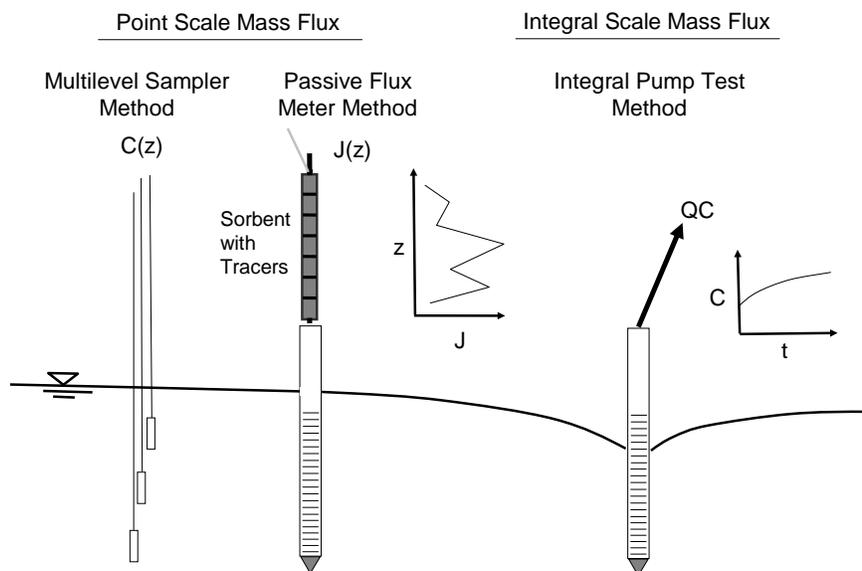

Figure 4.1 Point and integral mass flux methods in wells screens typically 5 to 30 feet in length and well spacing 10 to 50 feet.

Local measures of mass flux can be determined from local flux average concentration, local hydraulic conductivity, and the local head gradient applied in the maximum flow direction, but typically average values are used for hydraulic conductivity and the head gradient. Spatial variability is obtained from the concentration distribution, determined using multilevel samplers.

a. Transect Method

The transect method calculates contaminant discharge using the product of the well cross sectional area within a transect of wells, the contaminant concentration, and the Darcy flux. The Darcy flux is the product of the hydraulic gradient and the hydraulic conductivity. Average values are used for the hydraulic conductivity, the hydraulic gradient, and the flux averaged concentration that is collected from each well. The contaminant flux is the product of the Darcy flux and the concentration collected from each well. The contaminant flux has spatial variability, so the local value may be significantly different from the average value. Integral values are assumed to be acceptable for calculating average fluxes and integrated fluxes over the well transect, but this assumption has not been tested in field sites.

The transect method can also be applied to areas down gradient of the source area or across a plume, using the local mass flux and local contaminant concentration. The Darcy flux can only be calculated if the local independent values are measured. The local hydraulic conductivity can be measured from borehole flow meter tests or slug tests, but typically average values are used. The local hydraulic gradient is rarely determined, so average values are used from monitoring wells.

The well-established methods used to collect data offer an advantage. The transect method also provides spatial information, and it incorporates infrastructure already present at the site all while producing minimal waste.

The transect method's disadvantages include the necessity of independent measures for the Darcy flux, and the possible errors arising from sampling small volumes of groundwater, and in order to reduce these errors more measurements must be taken. Low gradient systems can introduce errors for independent measures of flux since there is a small volume of groundwater being measured at one point in time, so data must be integrated to obtain contaminant mass loads. A study by Kubert estimated a range of 20 to 50 percent error for the transect method when the "plume" covers a relatively large portion of the control plane. A recent study using multilevel transects contained a larger margin of error than an integrated pump test.

b. Passive Flux Meters

Passive Flux Meters (PFM) use a sorbent pack that covers the vertical extent of the contaminant plume, and they allow the natural gradient groundwater flow during a designated time period to capture dissolved contaminants. At the time of placement, PFM are pre-saturated with "resident tracers." During the process, groundwater fluxes are calculated from the amount of depleted tracer mass, and contaminant fluxes are calculated from the amount of contaminant mass captured. The vertical profile of the PFM allows for a depth distribution to be determined.
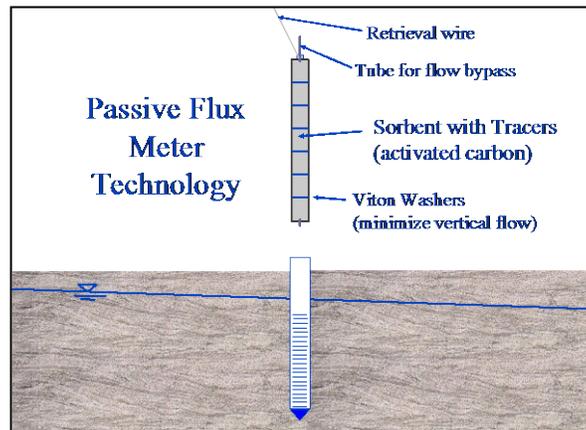
Figure 4.2. Installation of the passive flux meter in a screened well.

Existing site conditions allow estimation for groundwater flux and contaminant concentrations, which may help to select appropriate tracers so that tracer loss and contaminant mass accumulation are quantifiable.

The PFM method allows spatial information to be collected, integration of information over time can be done, and there is little error in integrated mass load. Based on measured hydraulic gradients, aquifer conductivity can be determined from this method. Minimal waste is produced, and this method can be applied in remote settings.

The PFM method does not take into account large volumes of the aquifer, so the error margin may be large. The data must be integrated in order to determine contaminant mass discharge and total water discharge. Tracers that are required must be approved for use in the subsurface, and PFM have not been applied to fractured media environments.

This approach has been implicated in over 40 sites, with the largest at Ft. Lewis, Washington, USA, where a PFM of 700 linear feet was deployed in 10-well transects. The deepest application took place near Perth, Australia at 67 meters deep.

c. Integral Pump Tests

The integral pump test (IPT) places multiple pumping wells perpendicular to the direction of groundwater flows and measures contaminant concentration-time series. The measured concentration of contaminants is used with the natural gradient Darcy flux in order to determine mass flux or discharge. The significant volume of water allows an integral measure of contaminant concentration along the well transect, and avoids missing "plume cores" within the transect.

The IPT estimates contaminant mass flow as well as supplies information on the spatial distribution of mass flux across the well transect. This approach can be applied to deep aquifers, and has no limitations based on well design.

The IPT generates a large volume of waste that can be costly depending on site infrastructure. Tandem circulation wells have been applied in some sites in order to overcome this challenge. The deployment time can be lengthy, and the method requires independent measures of the Darcy flux.

6. Ft. Lewis DNAPL Case Study for Mass Flux Evaluation

The data collection at Ft. Lewis demonstrates a DNAPL contaminated site with extensive characterization and source remediation in which flux assessments were used. The purpose of the data is to look beyond remedial performance assessment in order to see how the data would benefit remedial design and site management.

The Ft. Lewis TCE contaminant plume is 3 km long with a source zone at the East Gate Disposal Yard (EGDY). Three primary contaminated regions were identified and evaluated for a variety of remedial technologies; resistive heating was selected. Thermal Remediation Systems (TRS) was used over a period of 3 years, starting with NAPL Area 1, the most upgradient source. The focus of remedial assessment using flux data was on NAPL Areas 1 and 3, and NAPL Area 2 was not evaluated by pre- and post-flux measurements, but alternative measurements were taken.

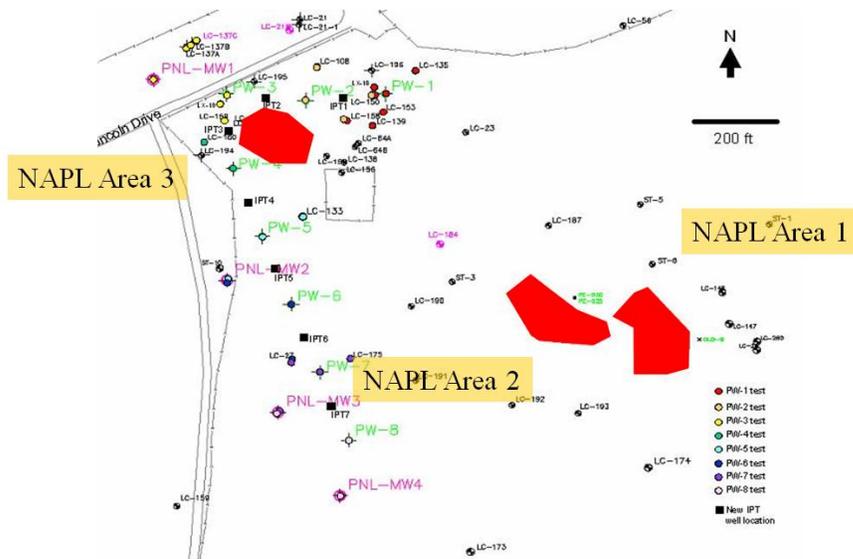Figure 4.3. TCE contaminant plume at Ft. Lewis c. 2003.

Figure 4.4. Ft. Lewis NAPL treatment areas.

The EGDY source areas 1 and 3 were evaluated in order to quantify mass flux and integral mass discharge. A single transect of 10 wells were located immediately down gradient of treatment zone 1. Since zone 3 contained mass entering from up gradient sources, a transect of 8 wells was constructed immediately up gradient of the treatment area. Two transects of 10 wells were constructed immediately down gradient of zone 3 in order to cover the saturated thickness of the surficial aquifer of 50 ft.

The mass discharge was evaluated for its' effect on the entire plume system. A site wide integral pump test was conducted immediately down gradient of the source area; the test contained 15 fully screened wells and was conducted just after conductive heating of area 2. The measurements represent an intermediate mass discharge value that was impacted by remedial efforts in Areas 1 and 2.

The three well transects contained passive flux meters followed by integral pump tests. The IPT initial samples represent low flow samples of the fully screened wells, and were used to calculate mass discharge based on the traditional transect method. There are three approaches for quantifying mass discharge for each flux measurement, and each approach reports values for individual wells within the transect. The values are summed to quantify mass discharge.

a. Mass Balance Considerations

Mass distribution within the source area and within the plume is important for analyzing projections of mass discharge and for considering short term and long term site management. Initial mass estimates for the site were 11800, 13400, 43100 Kg of TCE for each of the three areas. Resistive heating removed 2580, 1090, 840 Kg, which demonstrated that the initial estimates were

high for the treatment areas due to the fact that diminishing returns were observed for the mass recovery, which suggested that high fractions of the original mass were removed. Mass removals during resistive heating are considered to be more reliable.

Mass discharge from NAPL Areas 1 and 3 estimate mass discharge history for each of the treatment areas, based upon certain assumptions. The observed mass discharge measured at NAPL Areas 1 and 3 were 6700/7300 mmoles/day, nd 2300/8800 mmoles/day. A model must be assumed, and the simplest model is an exponential decay model. The mass at the beginning of the treatment was 2600 KG, and the mass after treatment was 19 Kg, resulting in a removal of 99.3%. An initial date of 1950 was assumed, and an initial mass in NAPL Area 1 was estimated as 5200 Kg. The same analysis for Area 3 resulted in an initial mass of 2800 Kg. Based upon mass removal, NAPL Area 2 was estimated to have an initial source mass of 3100 Kg. The total initial estimate of 10,000 Kg of TCE is calculated, and approximately 5000 Kg present in the dissolved plume.

A site wide IPT conducted 6 months after heating was terminated in Area 1 provides valuable insight on the site-wide mass balance. The northern and central sections can be compared with NAPL Area 3. The site-wide IPT mass discharge of 3450 mmoles/day compared with 3200 mmoles/day, whereas the PFM resulted in 8800 mmoles/day. NAPL Area 1 must be summed with an unknown estimate from NAPL Area 2 to estimate the site-wide mass discharge prior to treatment since NAPL Area 2 is down gradient from NAPL Area 1, and the mass discharge may be reduced due to the presence of TCE in solution from NAPL Area 1. Two alternate cases may be considered; no additional mass can be accounted from NAPL Area 2, or NAPL Area 2 contributes a scaled mass input based on results from other zones. These two cases result in a mass discharge of 11000 to 14000 mmoles/day.

b. Remedial Design Considerations

NAPL Areas 1 and 3 were evaluated for local flux measurements using transects of wells using PFMs segmented in vertical intervals of 30 cm. At the down gradient section of NAPL Area 1, each well contained a vertical flux profile of 25 samples. The data along the transect was used to produce a contour plot of the flux distribution, and the data demonstrated the variability of TCE mass flux emanating from the DNAPL source area. The majority of the mass flux is localized within the control plane, but there are likely individual pools of DNAPL located up gradient. In NAPL Area 1, about 90% for the mass flux is contained within about 33% of the control plane. This demonstrated the mass is originating up gradient of the flux observation at the control plane, and can reduce the size of the remediation zone by focusing on the up gradient regions.
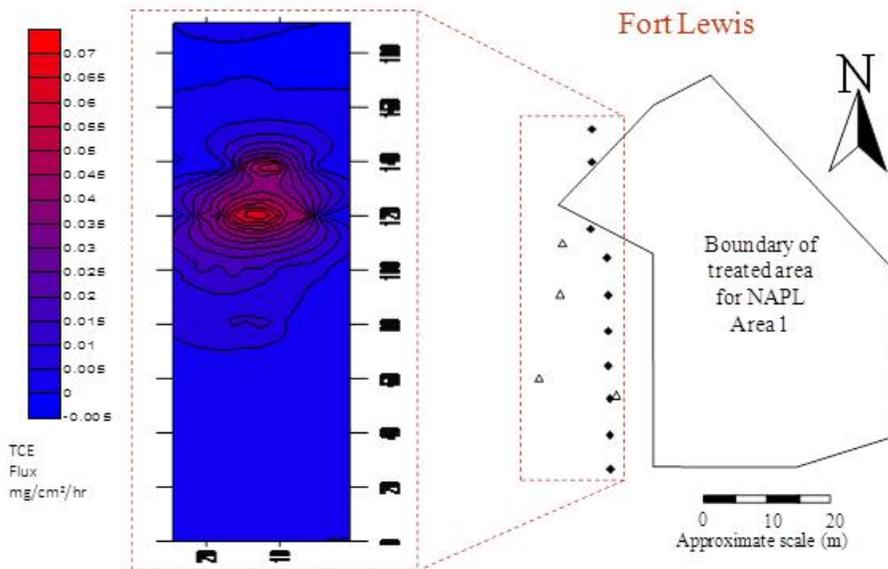
Figure 4.5.   Ft. Lewis NAPL treatment area 1.

The control plane flux data is considered an instantaneous measurement that is the result of groundwater flow imposed on the DNAPL source area for the travel time required between source and control plane, taken in the predominant direction of groundwater flow. The travel time for NAPL Area 1 is approximately the travel time through the treatment area, and the distance is about 50 m. PFMs estimate Darcy velocity of 0.25 m/day, and a porosity of 0.33, resulting in a travel time of 70 days. The predominant gradient from the past 70 days should be used to locate up gradient source areas. The average gradient magnitude and direction should be calculated, but this gradient may shift between wet and dry seasons so this must be considered when selecting when to collect measurements.

NAPL Area 3 was also evaluated both up gradient and down gradient for flux distributions, and contour maps were also made. The flux distribution up gradient was less localized than Area 1 most likely due to a larger travel distance between the source and the control plane which resulted in more mixing and dispersion.

Figure 4.6. Shallow down gradient mass flux distribution NAPL Area 3. Flux volumes are mg/m^2/d.

The down gradient control plane was 50 ft in saturated thickness which was much thicker than Area 1 which is the result of the till unit at the base of the surficial aquifer. The flux distribution is more localized.

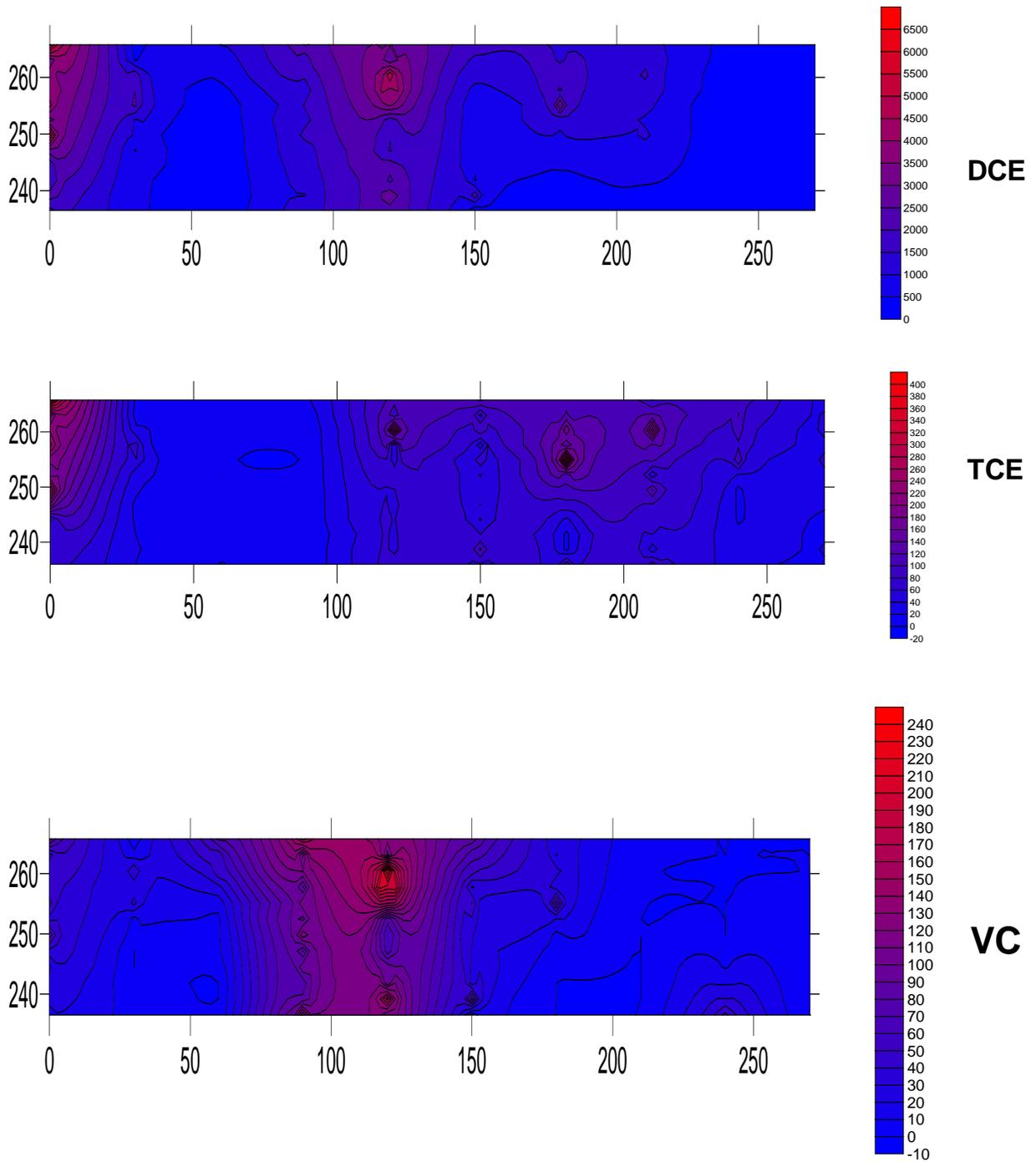# 7. Borden Coal-Tar Emplacement Experiment Case Study for Mass Flux Evaluation

Chlorinated solvent DNAPL sites have been the focus of mass flux evaluation; however the same concepts can be applied to manufactured gas plants (MGP) or other general contaminated sites with a source and a plume as well as decisions to best manage the site with limited resources. The relationship between the source strength and the rate of degradation represents whether a plume is advancing, receding, or is at steady state, and it can be applied to sites with monitored natural attenuation of polycyclic aromatic hydrocarbons (PAH).

There are differences between chlorinated solvent DNAPL sites and coat tar DNAPL sites, specifically the source function and one model that's been applied is the power law model (PLM). The PLM describes source function behavior with a screening-level mathematical description using the exponent, Γ, which is a function of the DNAPL spatial distribution, the hydraulic conductivity spatial distribution, and the correlation between the two. Dissolution behavior associated with multi-component NAPL is not accounted for in this model.

Results from a field experiment in August 1991 where 74 Kg of coal tar creosote was injected in a shallow aquifer at the Canadian Forces Base in Borden, Canada will be discussed. The source, plume, and recent results have been monitored. The emplacement involved mixing creosote above grade with ~5800 kg of coarse sand, then the material was placed below the water table in two 2m by 2m by 0.5 m blocks separated by 1m. The bulk saturation was about 7%.

It was assumed the DNAPL was uniformly distributed and had homogeneous hydraulic conductivity, which would theoretically create a source function in which the majority of the DNAPL would have to be depleted before reductions in source mass discharge occurred. This behavior represents a small PLM exponent. Individual components in a multi-component DNAPL behave very differently even though a multi-component DNAPL as a whole behaves similar to a single component DNAPL.

One relationship used to describe dissolution from a multi-component DNAPL is Raoult's law (Banerjee, 1984), which states that dissolution of the ith species is a function of the aqueous solubility and DNAPL mole fraction:

$$C_i = \chi_i \gamma_i S_i \quad , \tag{Eq. 18}$$

where C_i is the aqueous concentration [ML^{-3}] of the ith solute resulting from equilibrium partitioning from the DNAPL; χ_i and γ_i are the mole fraction [-] and the activity coefficient [-] of the ith solute in the organic phase, respectively; and S_i is the pure-phase aqueous solubility limit [ML^{-3}] of the ith solute. Often γ_i is assumed to be 1, which is the value in an ideal organic fluid. Raoult's law has been applied to predict solute partitioning between coal tar and water. Measurements and estimates based on Raoult's law have been in agreement, with the difference ranging from factors of 2 to 4; others have noticed order-of magnitude differences or have noticed kinetic limitations in mass transfer between water and coal tar. Another method to predict solute partitioning between water and coal tar is polyparameter linear free energy relationships which uses a mechanistic description of the intermolecular interactions.

Raoult's law has been applied to the Borden emplacement study. The PLM can be applied for the source function using an exponent of 1 for more soluble compounds, but the less soluble compounds in the early time data deviate from the PLM behavior due to the mole fraction increasing with time as more soluble compounds leave the DNAPL. Any less soluble compound becomes more soluble after some time, and its dissolution follows a PLM with an exponent of unity.
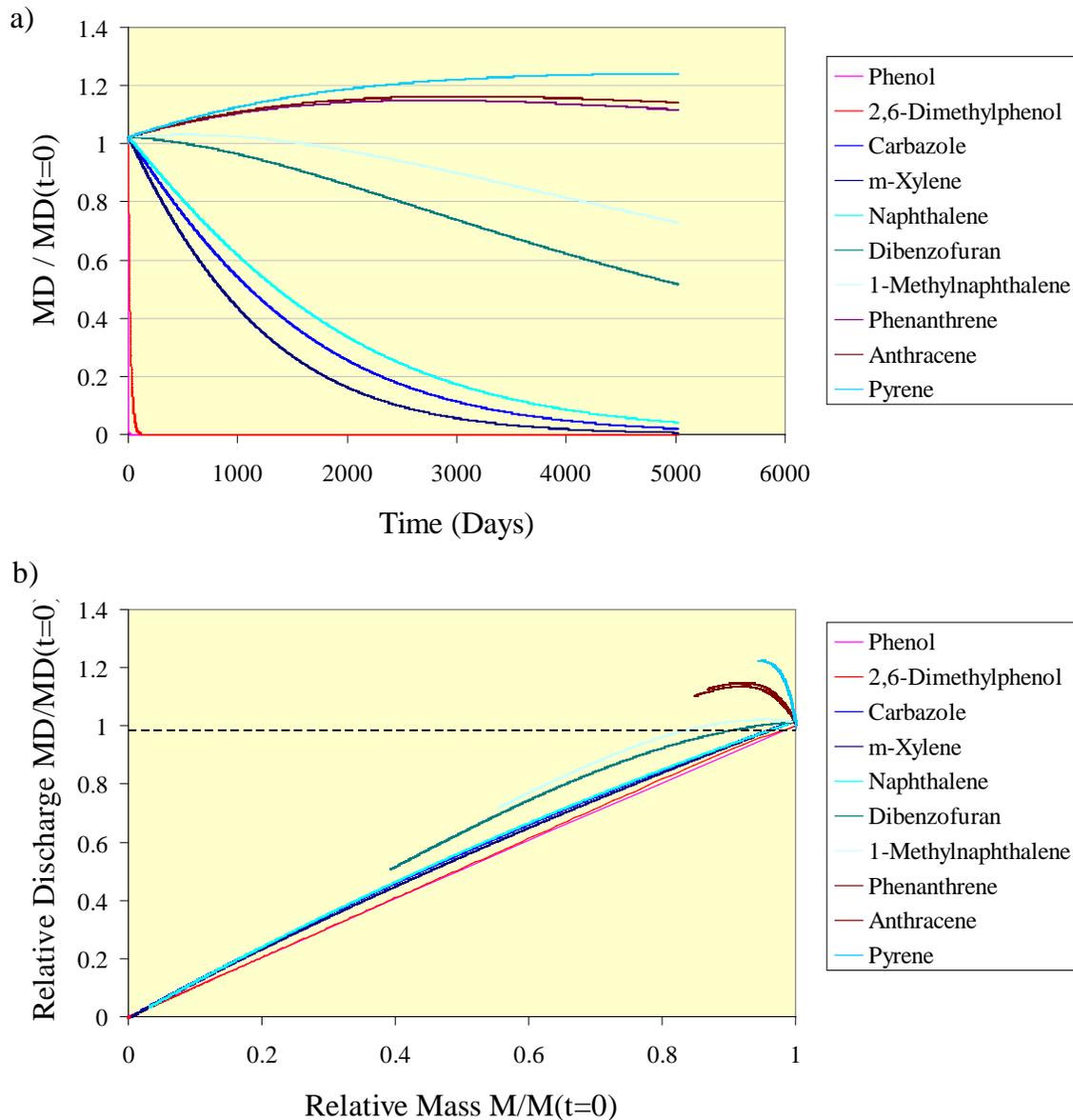

Figure 6.1. a) Source strength function (relative mass discharge versus time) for select PAH compounds based on Raoult's law and data from the Borden coal tar emplacement experiment, and b) source function (relative mass discharge versus relative mass) for the same

select PAH compounds based on Raoult's law and data from the Borden coal tar emplacement experiment (King and Barker, 1999).

Shown in Figure 7.10 is mass discharge, M_D, as a function of time for 10 compounds as reported by Fraser et al (2008); 6 measurements were completed between 278 to 514 days after emplacement. This data provides a useful opportunity to test how well simple models of source strength functions predict future behavior using intermediate scale pilot tests. It will be assumed that the first three measurements collected between 278 and 1357 days after emplacement, were part of site monitoring activities and will be used to make predictions of mass discharge. These predictions in turn are compared to measurements completed for $3619 \leq t \leq 5140$ days.
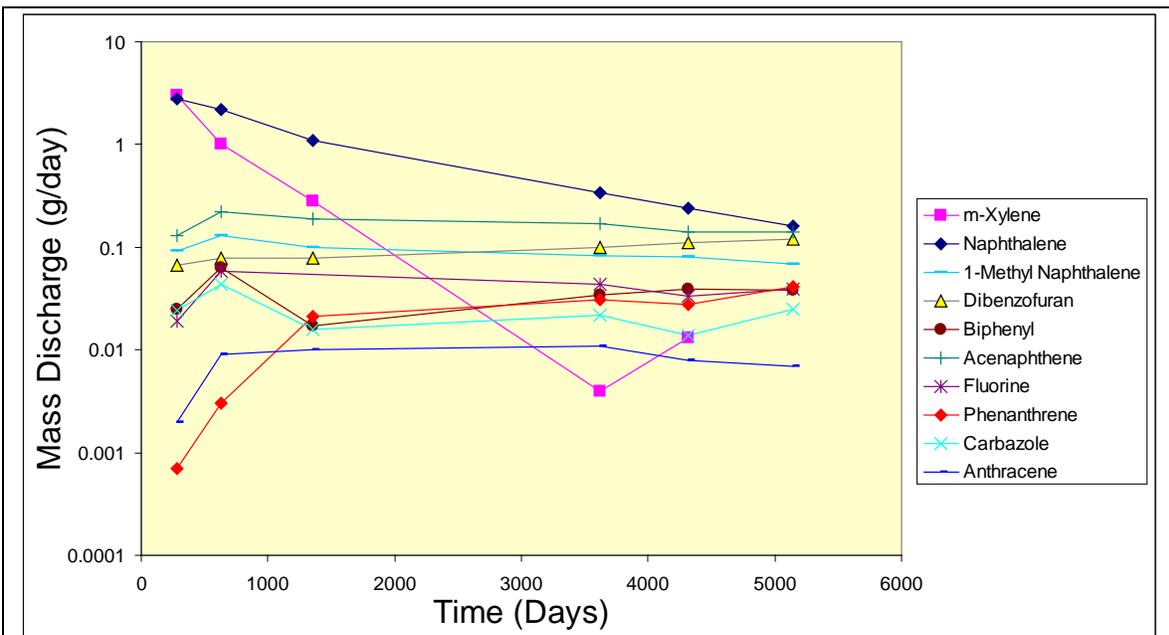
Figure 6.2. Source mass discharge (g/day) as a function of time (days) for 10 monitored compounds. Data reported by Frasier et al. (2008).

If the first three measurements are viewed in isolation, it would be assessed that monotonically decreasing trends in M_D are evident for m-xylene and naphthalene, while monotonically increasing trends in M_D are evident for phenanthrene and anthracene. With the exception of fluorine, mass discharge for the remaining compounds increase over the first two measurements, but decrease with the third. Results for fluorine were not reported for t = 1357 days, but M_D increased over the first two measurements. This behavior can be explained by the more soluble compounds leaving the NAPL which causes the mole ratio of the less soluble compounds to increase, resulting in a higher effective solubility. It is noted that the response at the source zone control plane is an integrated measurement process that represents dissolution as well as sorption/desorption processes between NAPL and the control plane, and potential mass loss.

M-xylene and naphthalene show decreasing trends that can be fit to the power law model. Model fits were completed for $\Gamma = \{0.5, 1.0, 2.0\}$ using linear regression, and are shown in Figure 7.11. For $\Gamma = 1.0$, a linear transformation of the mass discharge data is required prior to linear regression using the natural logarithm (i.e., $y = \ln[M_D(t)]$, where y is the transformed data upon which linear regression is completed). Likewise, for $\Gamma = 2.0$, a linear transformation of the mass discharge data is needed using the inverse of the square root (i.e., $y = M_D(t)^{-1/2}$), where y is the transformed data upon which linear regression is completed). As shown in Figure 6.3, the mass discharge measurements competed for $3619 \leq t \leq 5140$ days fall in between model fits for $\Gamma = \{1.0, 2.0\}$. The model fit using $\Gamma = 0.5$ results in the largest discrepancy between measured data and model predictions. However, the rapid decline in the source strength as predicted by a PLM with $\Gamma = 0.5$ is generally considered unlikely.
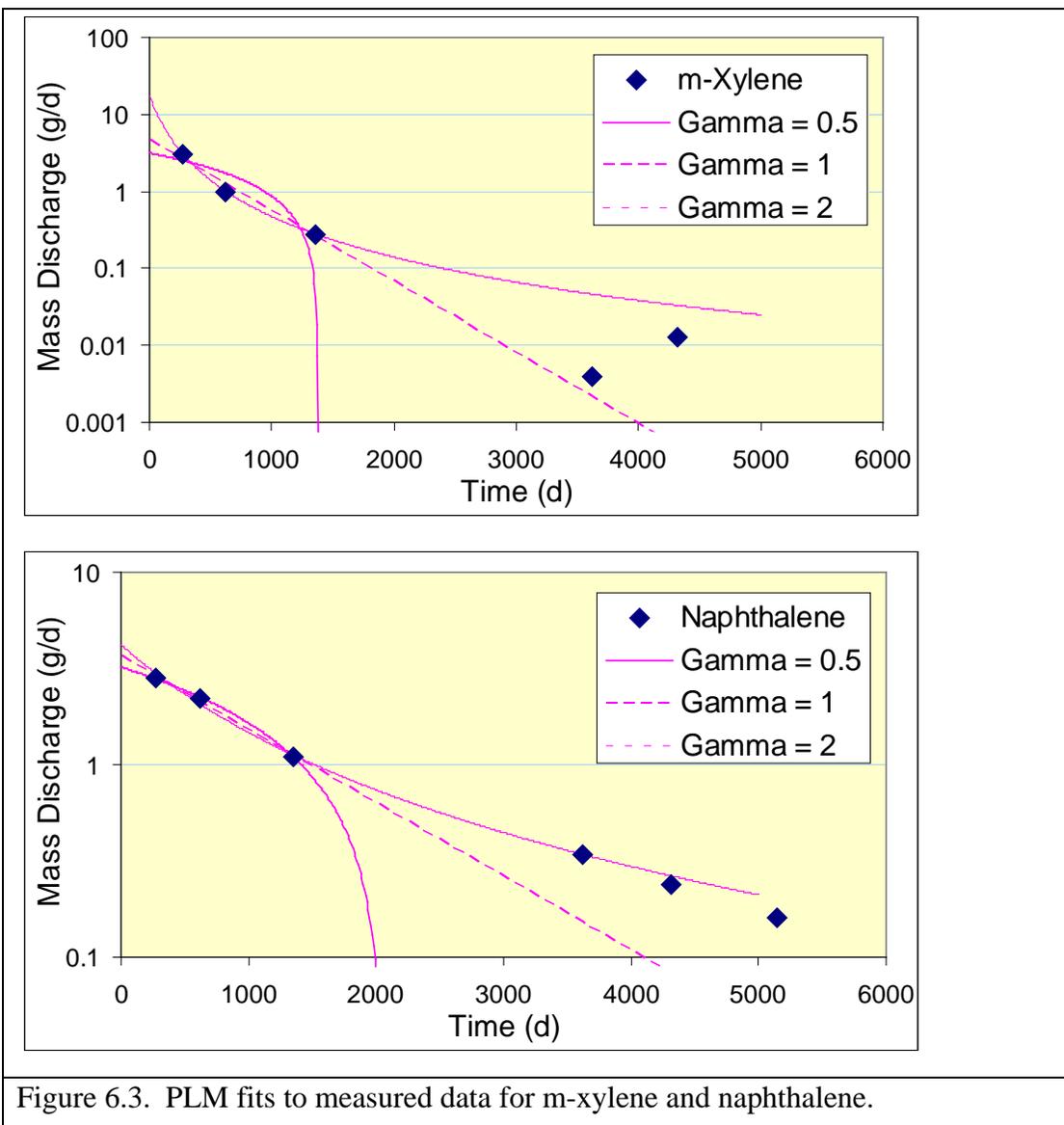

Figure 6.3. PLM fits to measured data for m-xylene and naphthalene.

a. Source Mass Estimation

Integration of core data, partitioning tracer tests, and geophysical methods have been used to estimate source mass; however estimates have high uncertainty due to spatial heterogeneity in subsurface characteristics and contaminants.

Once a PLM has been fit to the data, it can be used to estimate the initial source mass, M_0 (i.e. Eq. 7). For m-xylene, estimates of M_0 were {2170, 2204, 3441} g for Γ ={0.5, 1, 2}, respectively; while the emplaced mass of m-xylene was 2850 g. Estimates of the initial mass were therefore within a factor of 2 of the true mass. For naphthalene, estimates of M_0 were {3298, 4176, 6076} g for Γ ={0.5, 1, 2}, respectively; while the emplaced mass of naphthalene was 7110 g. Estimates of initial mass were therefore within a factor of 2.2 of the true mass. For any field-based method of DNAPL mass estimate, these results have to be considered as very good. However, the controlled nature of the study may be responsible for the agreement between the estimates and the actual values, and applications of this approach to more complex field sites need further evaluation.

b. Borden Coal-Tar Plume Behavior

Evaluation of the plume behavior with respect to source strength and the attenuation capacity within the plume was important for flux based site management. Plume behavior for the first four years of the study was reported by King and Barker (1999) and King et al. (1999) for seven compounds: phenol, m-xylene, naphthalene, phenanthrene, dibenzonfuran, carbazole, and 1-methylnaphthalene. Phenol (reported solubility of 82,000 mg/L) was observed to completely dissolve from the source and migrate downgradient as a discrete slug, and was completely degraded after 2 years. For m-xylene and carbazole, the plume was observed to migrate downgradient and then recede as the mass flux from the source decreased below the natural attenuation capacity within the plume. The spatial extent of dibenzofuran reached steady state, indicating a balance between the mass discharge from the source and the rate of plume degradation. Napthalene and 1-methylnaphthalene continued to migrate downgradient over the entire study period, indicating source mass discharge exceeded degradation. The phenanthrene plume was also observed to expand, and recede, however the degree of sorption associated with this compound hampered assessment over the study duration. Fraser et al. (2008) extended the analysis presented by King and Barker (1999) and King et al. (1999) to a duration of 14 years, and included additional compounds in their analysis (anthracene, acenaphthene, biphenyl, and fluorine). The compounds were placed into one of three classes based on their plume behavior. The first class consisted of those compounds that were significantly attenuated over the 14-year study duration (phenol, m-xylene, and naphthalene), and represents the expected result when the natural attenuation capacity exceeds the source strength. The second class included the compounds for which the plume continued to expand over the entire 14-year study (phenanthrene and dibenzofuran), and represents the expected result when the source strength exceeds the downgradient natural attenuation capacity. The final class were those compounds that appeared to reach a steady plume extent (1-methylnaphthalene, carbazole, biphenyl, fluorine, anthracene, and acenaphthene), and represents the expected result when the natural attenuation capacity and source strength are balanced.

From the perspective of flux-based site management, and its application to future MPG sites, the Borden emplacement study highlights the dependence of the plume and its spatial extent on

the source mass, source age, source strength, and natural attenuation capacity. Manipulation of source mass and strength (through source remediation), or plume degradation (through plume remediation) are the options that can be used to optimize the management of the contaminated site if complete DNAPL source depletion is not feasible.

8. Alameda Site Case Study Using Source zone Capture Wells to Enhance DNAPL Dissolution

a. Short Term Pumping to Estimate Source Strength Function

The Alameda Site on Alameda Island located near San Francisco, California is a small, shallow DNAPL site contaminated with VOCs, mostly TCE, in the shallow aquifer. Research studies were conducted to create a conceptualized site model and to determine the source strength function (SSF) based on contaminant dissolution (see Wang et al., 2014). The study used historical groundwater data and membrane interface probes to provide an initial estimate of the extent of the DNAPL source. Soil cores, photoionization detectors (PID), and a hydraulic profiling tool (HPT) were also used to determine site characterization. The data showed the site contained a low flow zone from 4.6 m to 6.1 m, and a high flow zone from 6.1 m to 7.6 m.

Passive flux meters (PFMs) were installed into wills with screened intervals in both the low flow and high flow zone in the source zone in June 2010 with a vertical sampling resolution of 15 cm. MLS wells were also installed with a vertical sampling interval of 0.30 m, focusing on the low flow zone. A push-pull tracer test was conduction in August 2010 in two wells within the source zone, and one well in the plume.

Temporal DNAPL dissolution, also known as SSF, can help determine mass flux and mass discharge which can be applied to long term effects of source depletion efforts. The equilibrium streamtube model (EST) and the power law model (PLM) were two models that were applied to this site. The EST model is based on a Lagrangian approach where the DNAPL source zone is conceptualized as a collection of non-interacting streamtubes, with hydrodynamic and DNAPL heterogeneity represented by the variation of the travel time and DNAPL saturation among the streamtubes (Jawitz et al., 2003; Jawitz et al., 2005).

$$C(t) = \frac{1}{2} f_c C_s \left[1 - \mathrm{erf}\left(\frac{\ln t - \mu_{\ln \tau}}{\sigma_{\ln \tau} \sqrt{2}} \right) \right] \qquad \text{(Eq. 19)}$$

where $C(t)$ is the flux-averaged concentration leaving the source zone; f_c is the fraction of the streamtubes initially containing DNAPL; C_s is the solubility limit of the DNAPL in water; τ is defined as reactive travel time that combines the travel time t and the trajectory-averaged DNAPL content $\hat{S}$ ($\hat{S} = \frac{\hat{S}_N \eta}{\theta_w}$, where $\hat{S}_N$ is the trajectory-averaged DNAPL saturation along a streamline, η is the porosity , and θ_w is the water content); $\mu_{\ln \tau}$ and $\sigma_{\ln \tau}$ are the mean and standard deviation of the log normal variable $\ln \tau$. The travel time t and the DNAPL content $\hat{S}$ are both assumed to be lognormal variables, so the reactive travel time also follows the lognormal distribution.

The EST model is an accurate method of predicting DNAPL dissolution by using partitioning tracer tests (PTT) to independently parameterize the model. The initial aqueous concentration of DNAPL that is used to estimate f_c by dividing by the solubility limit and the nonpartitioning and partitioning tracers that show adequate separation are the data needed to parameterize Equation 1. Other tests such as soil cores, multilevel samplers (MLSs), passive flux meters (PFM) and push-pull tracer tests may be used to supplement the tracer data.

The PLM has been presented by Falta et al. (2005b), and Zhu and Sykes (2004),

$$C(t) = f_c C_s \left[\frac{(\Gamma - 1) f_c C_s V_d A}{M_0} t + 1 \right]^{\frac{\Gamma}{1-\Gamma}}$$ (Eq. 20)

where Γ is a PLM fitting parameter; V_d is the Darcy velocity; A is the cross-sectional area through which contaminants migrate; and M_0 is initial mass in the source zone. The special case of $\Gamma = 1$ leads to a simple exponential form for the source zone concentration over time (Zhu and Sykes, 2004),

$$C(t) = f_c C_s \exp\left(-\frac{f_c C_s V_d A}{M_0} t \right)$$ (Eq. 21)

In laboratory experiments, Chen and Jawitz (2009) found that dissolution follows an exponential decay at aged contaminated sites where a significant fraction of the initial DNAPL mass has been eluted from the source zone.

The volume of contaminant is difficult to know at DNAPL contaminated sites; however an estimate is essential to accurately estimate SSF parameters. Source mass was estimated using four methods (M1-M4). The first method used soil core data combined with membrane interface probe data (MIP) to delineate the extent of the DNAPL. The soil core data resulted in a high concentration of TCE (2200 mg/kg) at 5.8 m below ground surface (bgs), and (6600 mg/kg) at 6.1 m bgs. All other core samples were less than 100 mg/kg, which resulted in no DNAPL present. An approximate minimum (yellow circle area in Figure 7.1) and maximum (square area in Figure 7.1) extent of the DNAPL mass was delineated and the mass volume was determined using Equation 22,

$$V_N = \rho_b V_{soil} \overline{C} / \rho_{TCE}$$ (Eq. 22)

where ρ_b is soil bulk density and ρ_{TCE} is TCE density ; V_{soil} is volume of soil; $\overline{C}$ is average concentration based on the high resolution soil core at SPW-3-2 (mg/kg).

The second method used partitioning tracer test (PTT) data to estimate the average TCE concentration in the water swept volume based on the separation between two partitioning tracers that had different partitioning coefficients. The average saturation of TCE in the source zone can be estimated by the first normalized moment of the two partitioning tracers,

$$\overline{S}_N = \frac{R-1}{K_{N,2} - 1 - R(K_{N,1} - 1)}$$ (Eq. 23)

where the retardation factor, R, is the ratio of the first normalized moment of the partitioning tracers, K_N is the tracer TCE-water partitioning coefficient. The total DNAPL volume, V_N,

within the swept volume of each well was determined by multiplying the average $\bar{S}_N$ and swept volume V_S, determined for each well based on the first moment of n-hexanol tracer data which has a lower K_N to avoid the high uncertainties and complications using the recirculated methanol or IPA.

The third method used both tracer test and aqueous dissolution data during the push-pull tracer test and use of EST model theory to estimate DNAPL mass. The separation between the partitioning and nonpartitioning tracers for the push-pull tracer test was not distinct enough to directly estimate the DNAPL mass. An alternative approach was applied where the push-pull nonpartitioning tracer data (IPA) and contaminant dissolution data were scaled in order to make the solutes have similar radial travel distance and comparable relative concentration (Equation 6 and 7).

$$\bar{C}_{np} = 1 - \frac{C_{np}}{C_{0-np}} \tag{Eq. 24}$$

$$\bar{C} = \frac{C}{C_{peak}} \tag{Eq. 25}$$

where $\bar{C}_{np}$ is the normalized nonpartitioning tracer concentration; C_{np} is nonpartitioning tracer data during the push-pull tracer test; C_{0-np} is input tracer concentration; $\bar{C}$ is TCE concentration C scaled to the peak concentration C_{peak} during the push-pull tracer test. The separation between scaled nonpartitioning tracer data and dissolution data indicates the presence of DNAPL in the tracer swept zone and potentially can be used to estimate the mass in the source zone. The procedure proceeded by first fitting the scaled nonpartitioning tracer data to Equation 1 to determine $\mu_{\ln t}$ and $\sigma_{\ln t}$ by assuming no DNAPL ($\mu_{\ln \tau} = \mu_{\ln t}, \sigma_{\ln \tau} = \sigma_{\ln t}$), and then calculating the first moment of the t distribution m_1^t using,

$$m_1^t = \exp\left(\mu_{\ln t} + \frac{\sigma_{\ln t}^2}{2} \right) \tag{Eq. 26}$$

The peak scaled TCE dissolution data was fit to Equation 1 to determine $\mu_{\ln \tau}$, $\sigma_{\ln \tau}$, f_c and then calculated the first moment of the τ distribution m_1^τ using,

$$m_1^\tau = \exp\left(\mu_{\ln \tau} + \frac{\sigma_{\ln \tau}^2}{2} \right) \tag{Eq. 27}$$

Then, Equation 9 was used to calculated the first moment of the $\hat{S}$ distribution $m_1^{\hat{S}}$ (Basu et al., 2008a; Jawitz et al., 2003),

$$m_1^\tau = K_w m_1^t m_1^{\hat{S}} \tag{Eq. 28}$$

where K_w is equal ρ_{TCE}/C_s. The swept volume of the push-pull test was smaller than the source zone volume, but in this estimation, the same TCE distribution was assumed outside and within the push pull swept volume as in the source zone. Finally, the volume of DNAPL in the source zone was estimated using,

$$V_N = f_c V_{SZ} m_1^{\hat{S}} \tag{Eq. 29}$$

where V_{SZ} is the source zone volume (square in Figure 7.1) which is different from the swept volume V_S.

The fourth method used tracer peak concentration data during the PTT collected at the MLSs and also applied to the extraction wells. Here, a simple linear partitioning isotherm was assumed to partition tracer between the volume of water and volume of DNAPL in the MLS flow path as if the system was a batch reactor. Based on the partitioning relationship between NAPL and water phase, and mass balance of nonpartioning tracer (methanol) and partitioning tracer (2-octonal), NAPL volume was derived,

$$K_N = \frac{C_{p-N}}{C_{p-w}}$$

(Eq. 30)

$$M_{p-T} = C_{0-p}V_{in} = V_w C_{p-w} + V_N C_{p-N}$$

$$M_{np-T} = C_{0-np}V_{in} = C_{np-w}V_w$$

Combining these equations and rearranging produces

$$V_N = \frac{\dfrac{C_{np-w}}{C_{0-np}} - \dfrac{C_{p-w}}{C_{0-p}}}{K_{NW}\dfrac{C_{p-w}}{C_{0-p}}}V_w = \bar{S}_N V_w$$

(Eq. 31)

where C_{p-N} and C_{p-w} are tracer concentrations in the DNAPL and aqueous phase; M_{p-T} is the total partitioning tracer mass; M_{np-T} is total nonpartitioning tracer mass; V_w and V_{in} are volume of water, volume of DNAPL and tracer input volume, respectively.

M1 estimated volume at a range of 2 L – 20 L, which is a wide but reasonable range. M2 estimated 11 L overall, but had a retardation factor of 1.06 which is low because the overall saturation was low. The swept volume was 49 m³. The highest volume estimated was 5.8 L with a retardation factor of 1.12, but contains the highest uncertainties due to the retardation factor being below 1.2. M4-2 estimated 37 L of DNAPL, which is much greater than the 9.9 L estimated using the same method applied to the tracer data in the extraction wells (M4-1). M4-1 could have underestimated, or M4-2 overestimated the localized mass which produced larger peak differences. This method may not be representative of the entire source zone, and without the MLS PTT data, the volume of DNAPL in the low flow zone may not have been detected by other integral methods.
The site was estimated to be aged greater than 80% based on site mass balance. The initial mass was estimated using the methods presented, and using $\Gamma = 1$ as a good approximation. The EST used the parameters estimated by the PTT, and by fitting parameters using the equations presented and the push-pull tracer test. The aquifer and the TCE heterogeneity in the swept volume was assumed to represent the entire source area.

b. Use of Flux and Tracer Data to Improve Mass Balance

Predicting aqueous dissolution requires accurate mass in the source zone and in the fraction contaminated zone. The volume of contaminant is also required to predict SSF parameters. One method to calculate DNAPL volume is by using partitioning tracers. Particularly, the equilibrium streamtube model (EST) uses tracer tests to estimate parameters. Partitioning tracer tests, passive flux meters, multilevel samplers (MLS), and push-pull tracer tests may all be useful. The data collected from these tests during the early phase of site investigation provide essential data that can help delineate and confirm the extent of the source zone, and it can also be used to estimate source mass. All of the data combined can improve parameterization for the EST model.

Nonpartitioning tracer data can be used to estimate average travel time, travel time distribution, and to calculate the swept volume. Average pore velocities were estimated based on the partitioning tracer test nonpartitioning tracer (methanol) peak arrival time at MLSs. As discussed, the data demonstrated low flow zones, and high flow zones separated at a depth of 5.9 m below ground surface. Passive flux meters were installed into wells SPW-1, SPW-2, SPW-3, and SPW-4 with screen intervals in both the low-flow zone and the high-flow zone. Multilevel sampler wells were installed at locations SMLS-1 to SMLS-8 with a vertical sampling interval 0.30 m, focused on the low-flow zone. Passive flux meters were also deployed in the four extraction wells six and a half months after the end of the enhanced dissolution test. The velocity of the contaminant flow, as well as the source mass, allow more information to be applied to mass balance of the site.

Table 1. Well screen intervals and radius information in the source zone

Well	Screen Interval (m bgs)		Diameter (cm)
	up	bottom	
SIM 1~3	4.6	7.6	3.8
SMLS 1~8	5.0	7.0	1.3
PEW 1~4	4.6	7.6	10
SPW-1~2	5.2	6.7	3.8
SPW-3-1	5.2	5.9	3.8
SPW-3-2	5.9	6.7	3.8
SPW-4	5.2	6.7	3.8

Table 2. Tracer partitioning coefficient K_N (TCE –water) and input concentration C_0 for the push-pull tracer test and partitioning tracer test (PTT).

	Tracers	K_{NW}	C_0(mg/L)
Push pull tracer test	methanol	0	530
	IPA	0	1050
	n-hexanol	21	470
	DMP	63	540
	e-HEX	280	130
	1-octonal	421	130
Partitioning tracer test (PTT)	methanol	0	430
	IPA	0	1000
	n-hexanol	99	380
	2-octonal	266	120
	e-HEX	280	120

Table 3. NAPL volume estimates using four methods including swept volume, NAPL saturation and total mass volumes.

		V_{soil} (m^3)	V_N (L)		
M1	min	4.0	2.0		
	max	40	20		
		V_S (m^3)	R	$\overline{S}_N$	V_N (L)
	PEW-01	15	1.05	1.99E-04	3.0
M2	PEW-02	12	1.12	4.74E-04	5.8
	PEW-03	10	1.06	2.48E-04	2.5
	PEW-04	12	1.00	5.27E-06	0.06
	PEW-T	49	1.06	2.32E-04	11
		f_c	$m_1^{\hat{S}}$	V_S (m^3)	V_N (L)
M3	SPW-3-1	0.14	2.11E-03	12	3.7
		V_S (m^3)	$\overline{S}_N$	V_N (L)	
	PEW-01	15	1.38E-04	2.1	
M4-1	PEW-02	12	4.49E-04	5.4	
	PEW-03	10	2.06E-04	2.1	
	PEW-04	12	2.92E-05	0.35	
	sum	49		9.9	
	SMLS-4-1	1.15	0	0	
	SMLS-4-2	1.15	4.25E-03	4.9	
	SMLS-4-3	1.15	9.35E-03	11	
	SMLS-4-4	1.15	2.86E-04	0.33	
	SMLS-7-1	0.60	7.33E-03	4.4	
	SMLS-7-2	0.60	9.24E-03	5.5	
M4-2	SMLS-7-3	0.60	6.08E-03	3.6	
	SMLS-7-4	0.60	0	0	
	SMLS-8-1	0.30	9.96E-03	3.0	
	SMLS-8-2	0.30	9.37E-03	2.8	
	SMLS-8-3	0.30	6.81E-03	2.0	
	SMLS-8-4	0.30	0	0	
	sum	8.17		37	

Table 4. EST model parameters and volume of mass in the swept volume for each individual extraction well and flux averaged for all wells. The results are based on the best fit of the enhanced dissolution data (mass discharge) with the EST model using a generic algorithm code.

	E	f_c	$\mu_{ln\tau}$	$\sigma_{ln\tau}$	V_N(L)
PEW-1	0.93	0.016	3.50	1.32	2.6
PEW-2	0.80	0.024	3.85	1.33	5.5
PEW-3	0.92	0.010	3.60	1.47	2.1
PEW-4	0	0.001	5.0	0.20	0.49
Sum[*]					11
PEW-total[**]	0.90	0.013	3.66	1.41	11

[*] Sum represents adding mass volume from individual best fit for each extraction well;
[**] PEW-total used flux average mass discharge data from the four extraction wells to fit EST model and obtained mass volume directly.

Table 5. PLM parameters and volume of mass in the swept volume for each individual extraction well and flux averaged of all wells. The results are the best fit of the enhanced dissolution data (mass discharge) with the PLM using a generic algorithm. Well PEW-4 was manually fitted because the trend of data is not obvious and best fit could not obtained by using the generic algorithm.

	E	f_c	Γ	V_N(L)
PEW-1	0.94	0.016	1.064	1.9
PEW-2	0.81	0.026	0.94	3.1
PEW-3	0.92	0.010	2.44	2.2
PEW-4	0.0	0.002	0.01	0.49
Sum[*]				7.7
PEW-total[**]	0.90	0.013	1.28	7.8

[*] Sum represents adding mass volume from individual best fit for each extraction well;

[**] PEW-total used flux average mass discharge data from the four extraction wells to fit PLM model and obtained mass volume directly.

Table 6. EST model parameters used to predict aqueous dissolution

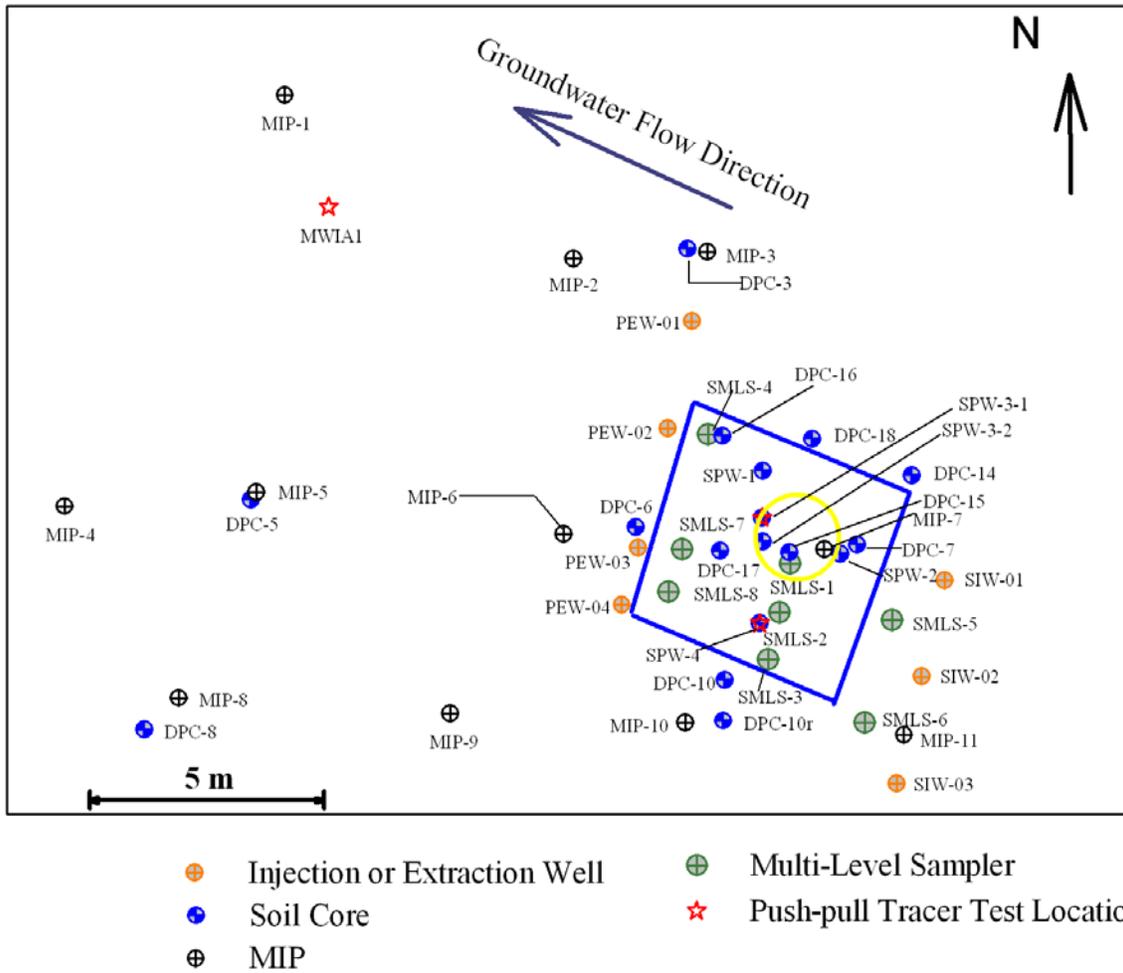| f_c	$\sigma_{ln\tau}$	V_{NAPL}(L)	$\mu_{ln\tau}$
0.010	1.4	2.0	2.43
0.010	1.4	20	4.29
0.010	1.4	11	3.73

Figure 7.1. DNAPL source zone and field activities. Soil cores at locations of PEW-03, SMLS-1, SMLS-2 and SIW-02 were also collected at locations where there were high PID signals. Note: dark blue square indicates the suspected source zone area, and yellow circle shows the minimum extent of TCE distribution with radius 1.2 m and thickness 1.4 m
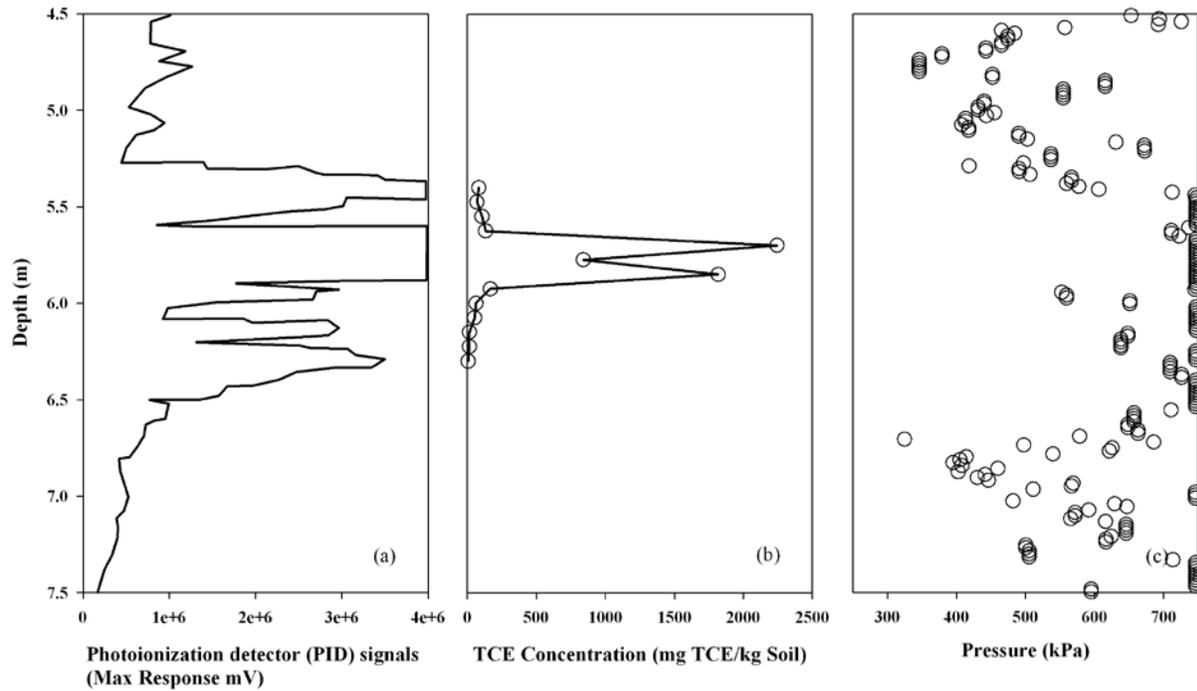
Figure 7.2. High DNAPL zone (a) MIP -7; (b) Soil core data at location SPW3-2; (c) pressure from a hydraulic profiling tool (HPT) located in the source zone. These three locations are close and potentially show high DNAPL zone at the depth of 5.2 m to 6.1 m within a low-flow zone.
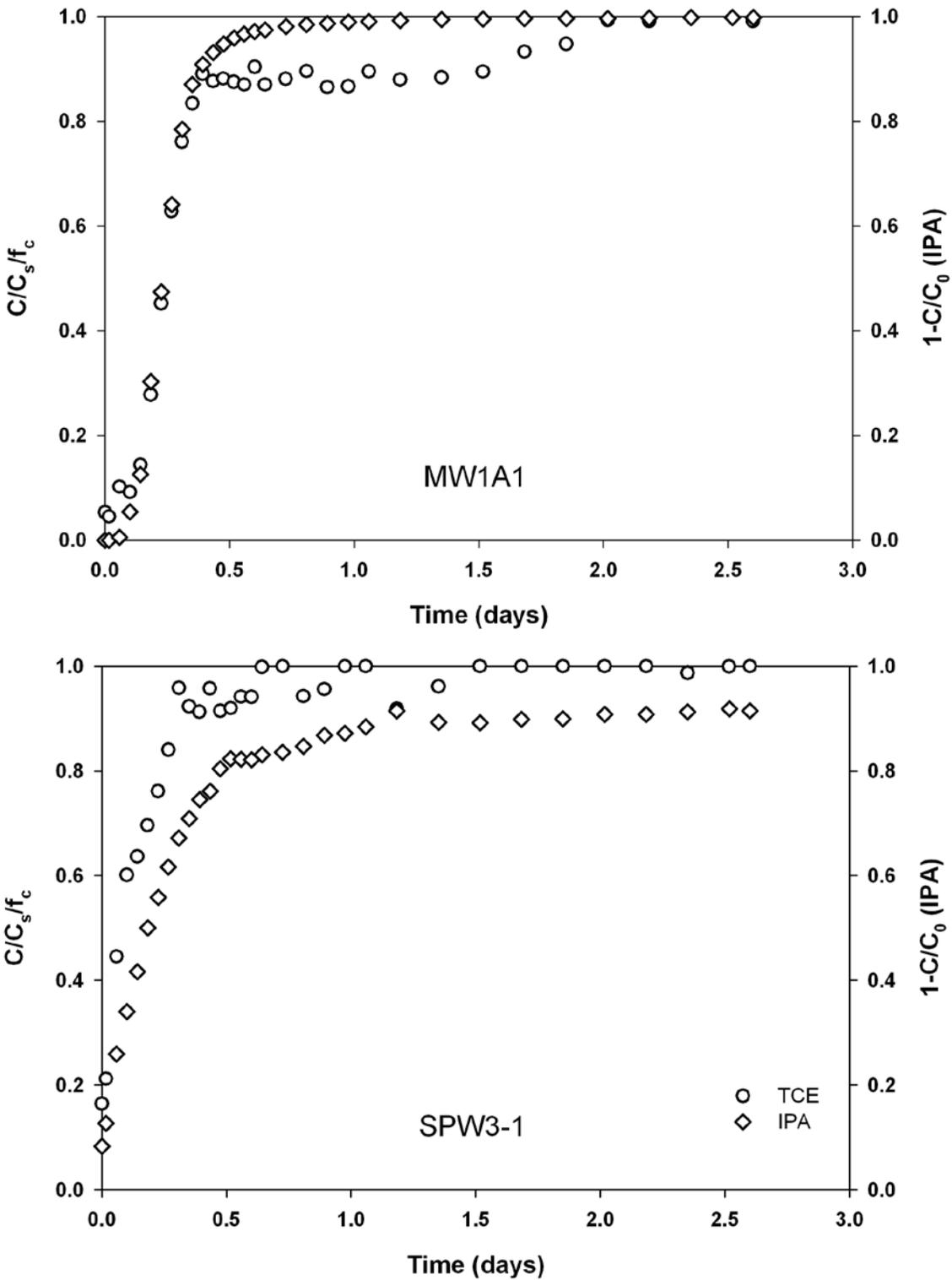
Figure 7.3. Arrival time comparisons between aqueous TCE and nonpartitioning tracer IPA during push-pull tracer test. The well MW1A1 is located in the plume and the well SPW3-1 is located in the source zone.
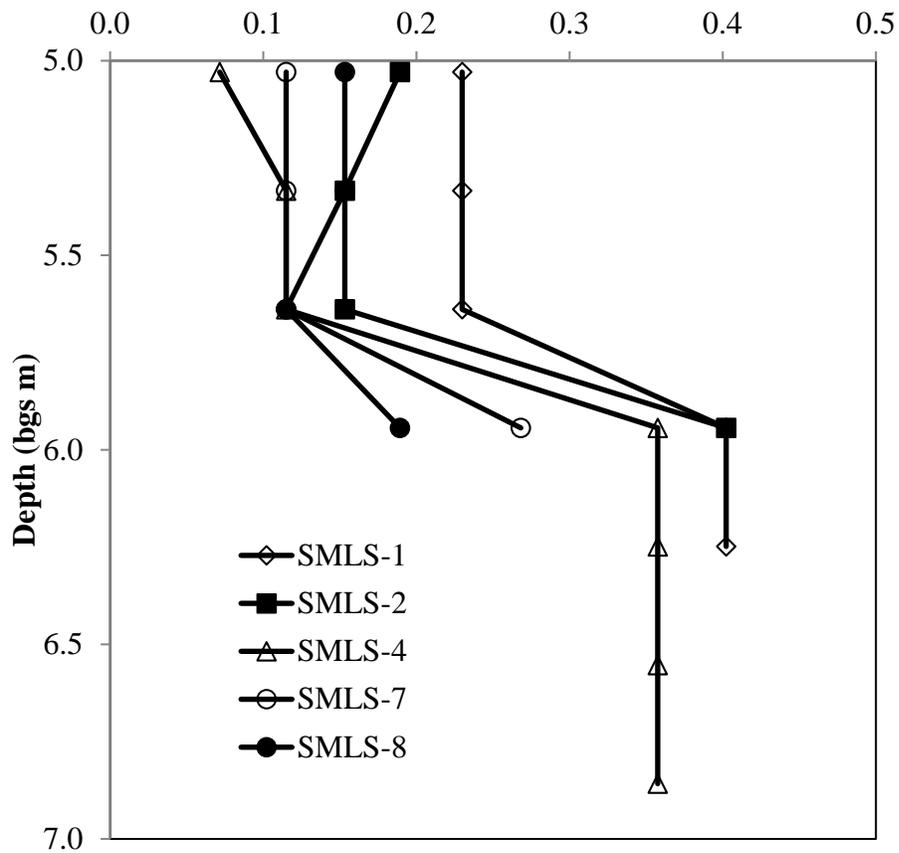
Figure 7.4. Pore velocity (m/day) versus depth for MLSs in the source zone during the PTT period. Pore velocity was calculated based on the distance from tracer release plane (SIWs) and nonpartitioning tracer (methanol) peak arrival times without considering tortuosity.
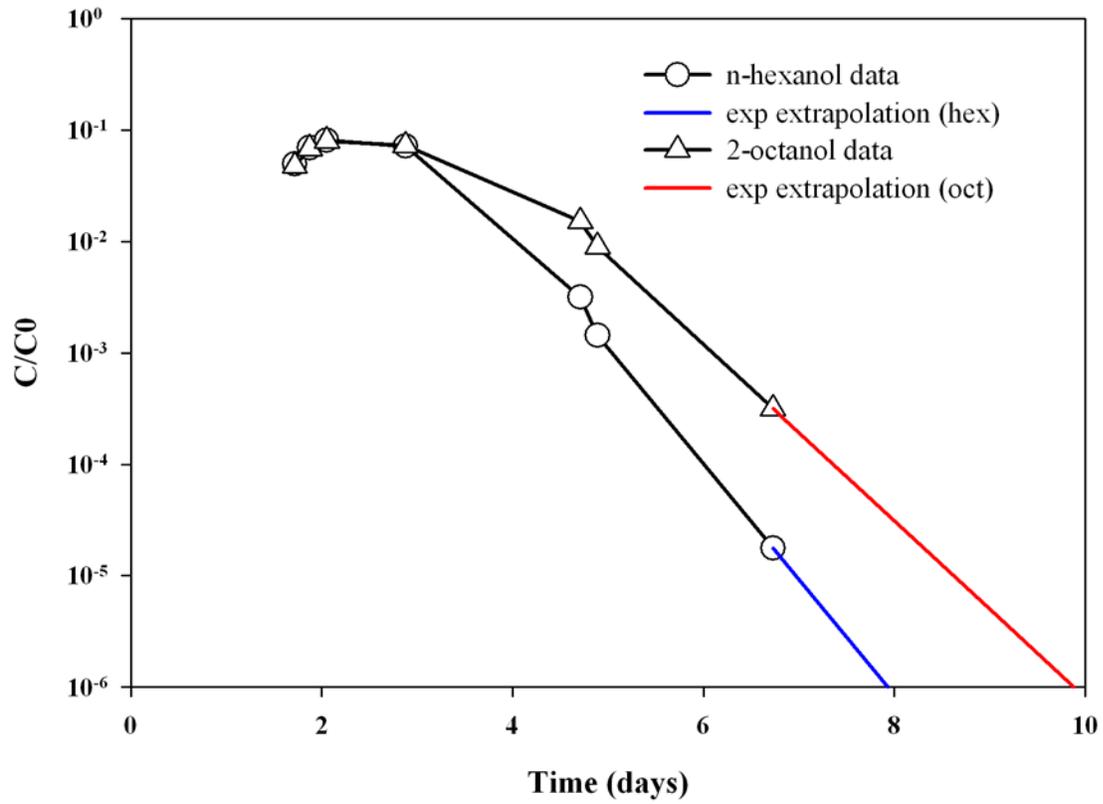
Figure 7.5. Partitioning tracer breakthrough curves for n-hexanol and 2-octonal with exponential extrapolations for the flow-weighted average PEW-T.
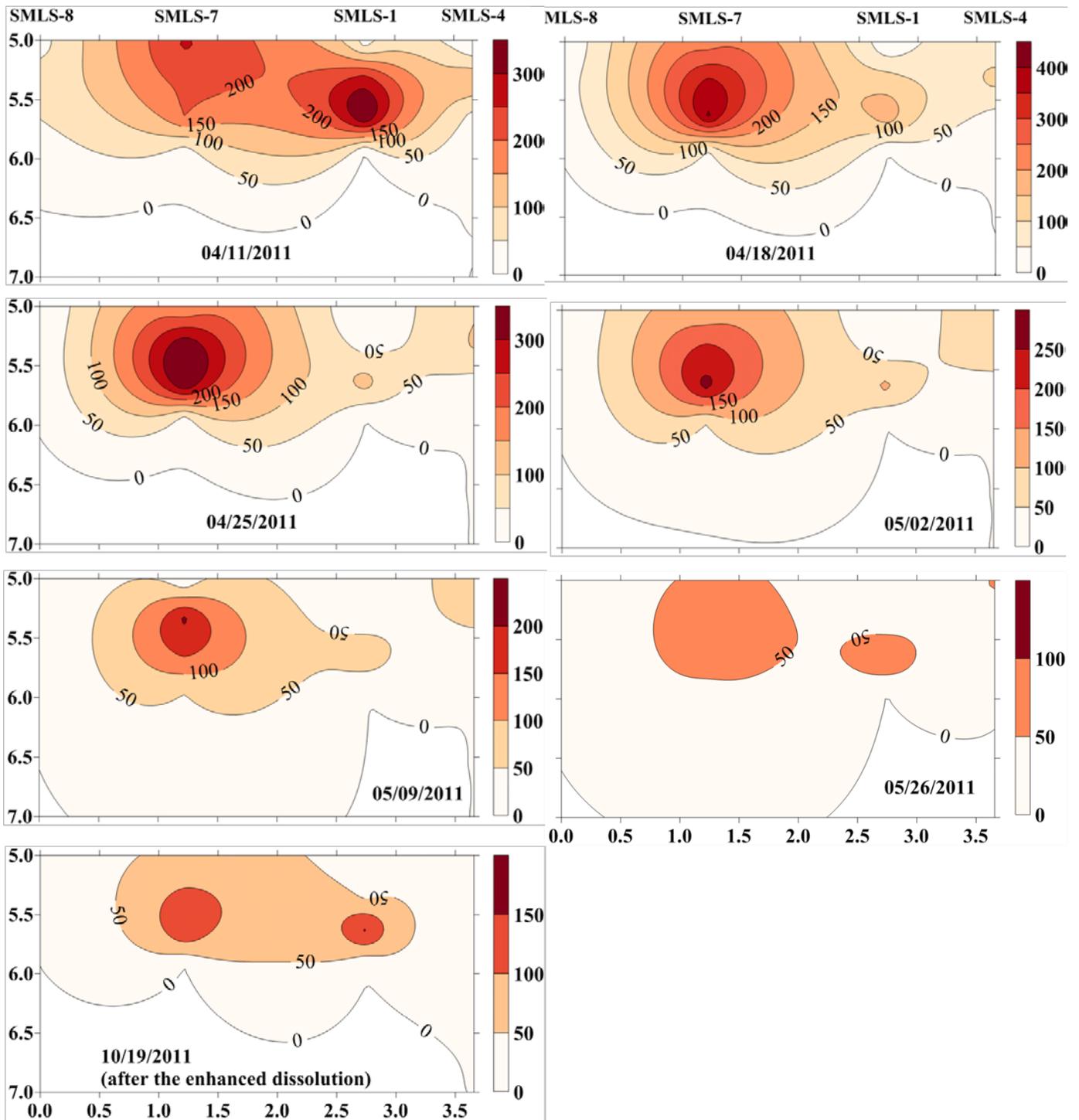
Figure 7.6. Aqueous TCE concentration during the enhanced dissolution and after the enhanced dissolution at SMLS-1, 4, 7, 8 transect.
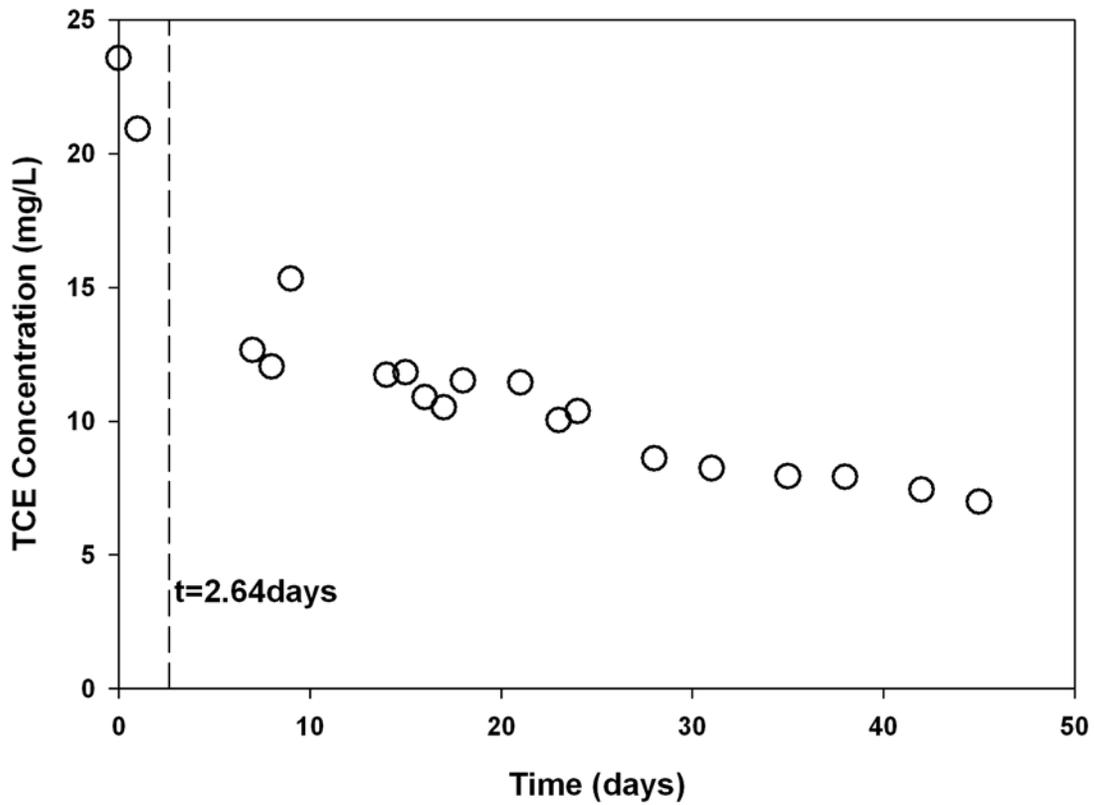
Figure 7.7. The capture time estimation for flux average TCE concentration from the four extraction wells. The dashed line represents the capture time (2.64days) when the flow approached steady state flow.
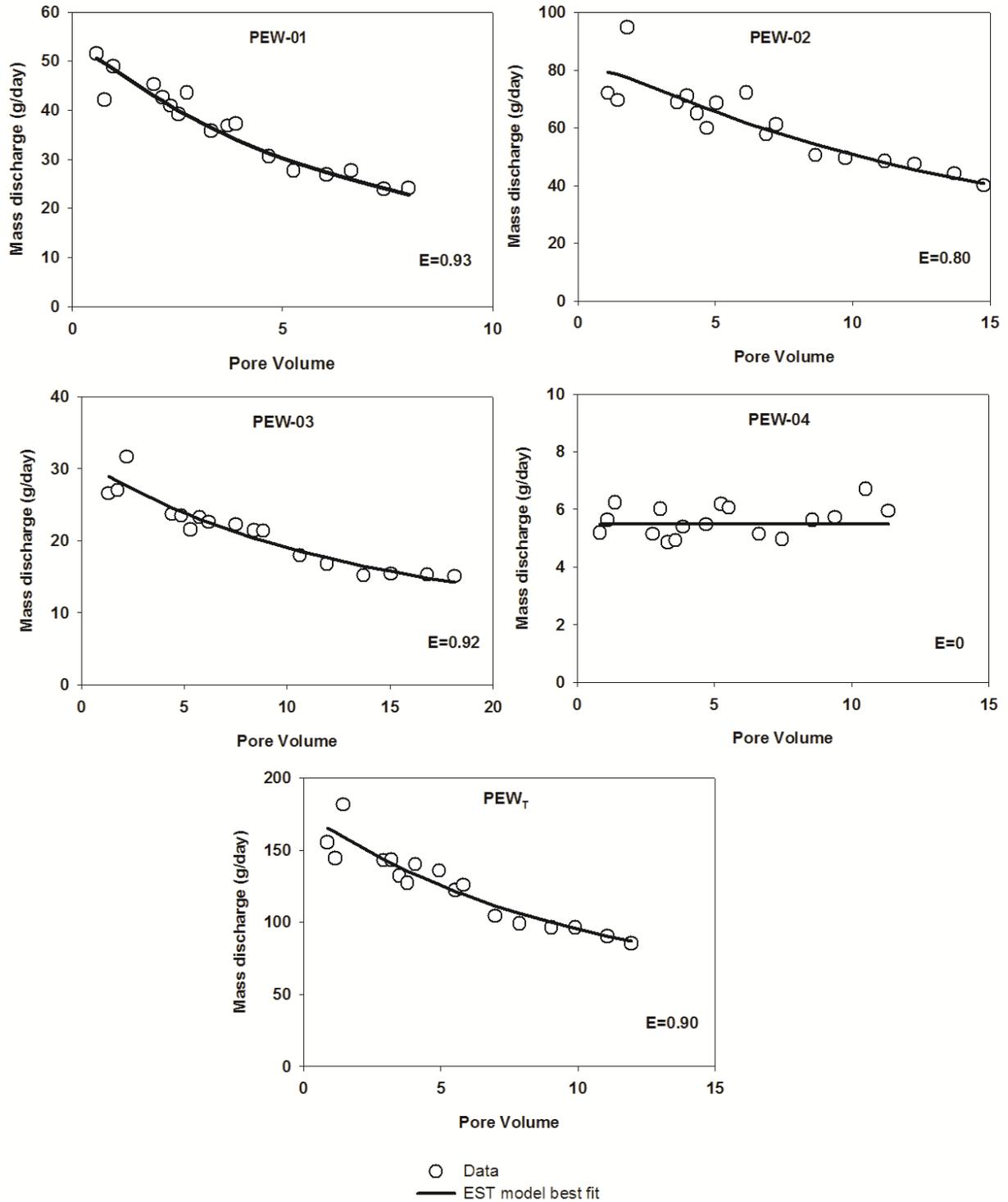
Figure 7.8. EST model best fit for enhanced dissolution data. Note: the pore volume zero represents the date for groundwater sampling before the enhanced dissolution.
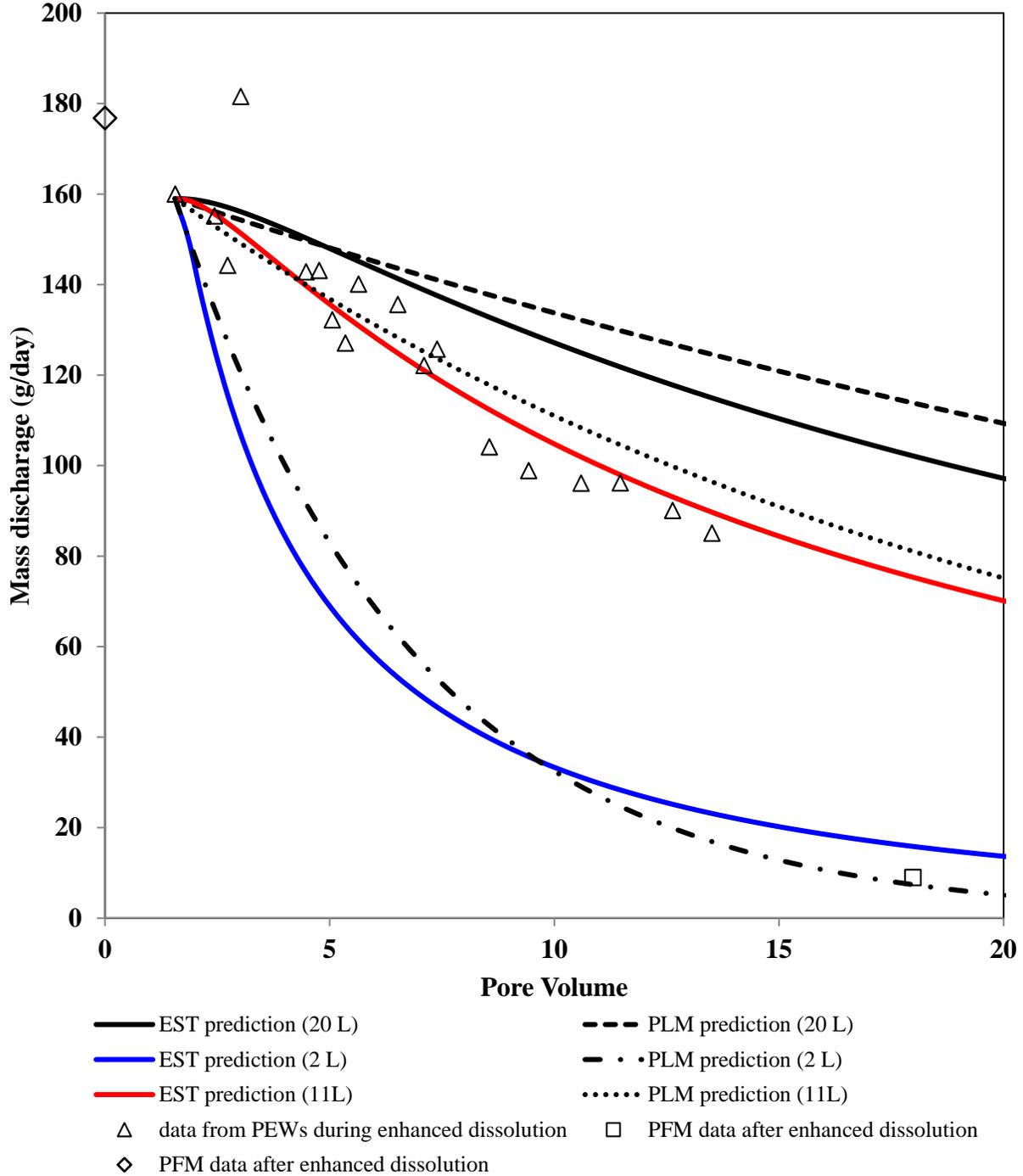
Figure 7.9. Aqueous dissolution predictions by combining soil core data, MIP data, Push-Pull tracer data and PTT data for both EST and PLM models. Passive flux meter (PFM) data before enhanced dissolution (diamond symbol) and after enhanced dissolution (square symbol) were plotted.

9. Calf Pasture Point Assessment using Spatial and Temporal Transects within the Plume

a. Evaluation of Source Strength Function

An understanding of the source-strength function is important because of its use in predicting responses to various remedial approaches, and therefore is a valuable tool for site management. In the Calf Pasture Point site study, the initial contaminant is estimated to be about 7,500 gallons of decontaminating agent non-corrosive (DANC) buried in drums. The composition of DANC is predominantly 1,1,2,2-tetrachloroethane (PCA) with an estimated release mass of 45,000 kg, but this estimate has a high uncertainty. PCA typically degrades rapidly to trichloroethylene (TCE), which is the predominant contaminant.

Wells are located throughout the site, and the focus is on the wells screened across the lower silt and till units (D-series wells) since they contain the highest concentrations. An analysis of the groundwater flow field was also conducted and shown in Figures 8.1 and 8.2.
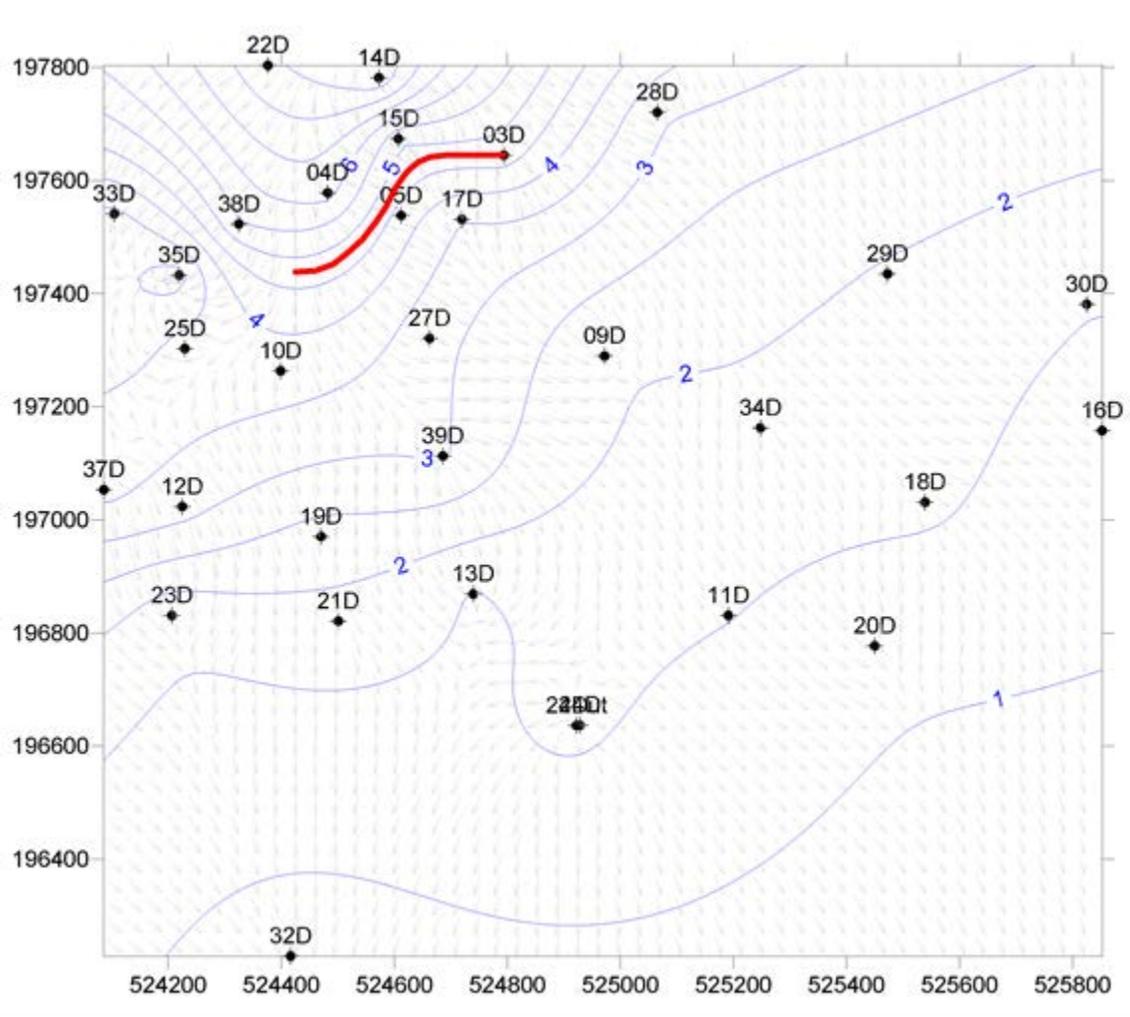

Figure 8.1. Groundwater elevation contour map based on average groundwater elevation measurements. Blue lines represent contour elevations in feet above mean sea level, and the

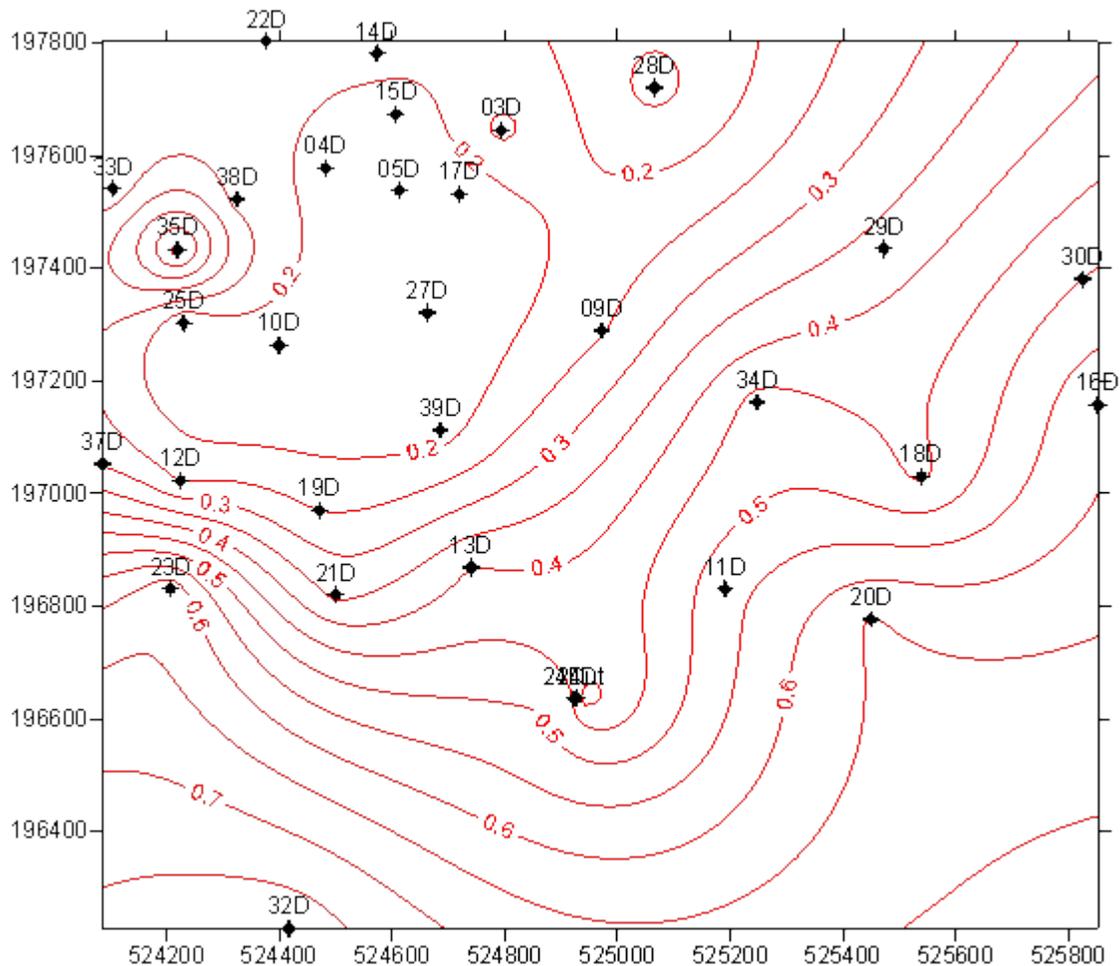grey arrows represent groundwater flow directions. The bold red line represents the curvilinear SZCP.

Figure 8.2. Coefficient of variation for groundwater elevation measurements.

The source-zone control plane (SZCP) is a control plane that measures the mass discharge of DNAPL immediately down gradient from the source zone. The estimation of mass discharge as a function of time can also be called the source-strength function.

The location of the SZCP impacts the source-strength function, and the SZCP has high uncertainty since the limits of the source zone have not been determined through source-zone characterization. The location of the SZCP was based on wells with long-term monitoring data, the proximity of the wells to the inferred DNAPL release location, and the location of the wells relative to the groundwater flow field. The spacing of the wells is roughly 90 feet. Well spacing has a large impact on the uncertainty of the estimated source strength function. The larger the well spacing, the greater the uncertainty will be. Variability in concentration with depth, and groundwater flux with depth impact the contaminant flux distribution. The travel time was

estimated to be 20 years, but other evidence suggests the travel time is most likely less than estimated.

Concentration-time series information from wells 04D, 05D, and 17D was used to estimate the source-strength function. Combining this information with well specific groundwater flux, contaminant flux was estimated which was then applied to calculate the mass discharge. The PCA was converted to TCE on a molar basis to calculate mass balance since TCE is the predominant contaminant. Mass discharge ranged from 300 g/day in 1996 to 50 g/day in 2010. The Power-Law Model was used to related DNAPL mass in the source zone to mass discharge from the source. The first measurements used for the model were from 1996. Certain calculations from October 2008 were completed, but not all calculations were included.

The Power-Law Model can also be used to estimate mass in 1968 by extrapolating data from 1996 under the assumption that the model does not change with time. Two cases were considered: the parameter $\Gamma = 0$, so the mass discharge over 42 years would be 4,600 kg, and the parameter $\Gamma = 1$, so the mass discharge over 42 years would be 22,400 kg. The first case resulted in a mass discharge that should generally be three times greater. The second case is more likely within the plume mass estimates, but the mass discharge in 1968 would have been 6,300 g/day which is higher than expected, but not impossible.

Mass balance requires that the mass discharged from the source zone equal the mass within the plume, plus any mass that may have been degraded. Plume mass estimates are useful for source strength function evaluation. Sorbed mass is accounted for using an estimate of the site specific retardation factor, $R = 7$. Since PCA degrades to TCE, which then degrades to DCE, the degradation is accounted for by using the molar sum of all three contaminants. The estimates for the source zone mass are roughly 100-300 kg PCA, and the plume mass is roughly 13,000-20,000 kg PCA, TCE, and DCE. The ratio of contaminants in the source zone to the mass in the plume is the site age, and thus this site is a relatively aged site.

Three transects were formed to conduct mass flux and mass discharge calculations based on PFM deployments. Approximately 90 PFMs were deployed in three transects to estimate mass discharge. The contour plots of mass flux are provided. These were used to calculate mass discharge at each transect and it can be observed that mass discharge increases along the length of the plume thus suggesting an exponential decay model may be appropriate for the source strength function. This can be estimated based on the observed data.

The longevity of the DNAPL estimated to remain within the source zone can be evaluated using a first order degradation analogy. The Power-Law Model using $\Gamma = 1$ is a good estimate, but this does not include other factors that may prolong contaminant mass in the source zone.

Recommendations for future work are also included in the next section. The recommendations are designed to minimize uncertainty with this analysis, and future site management decisions.

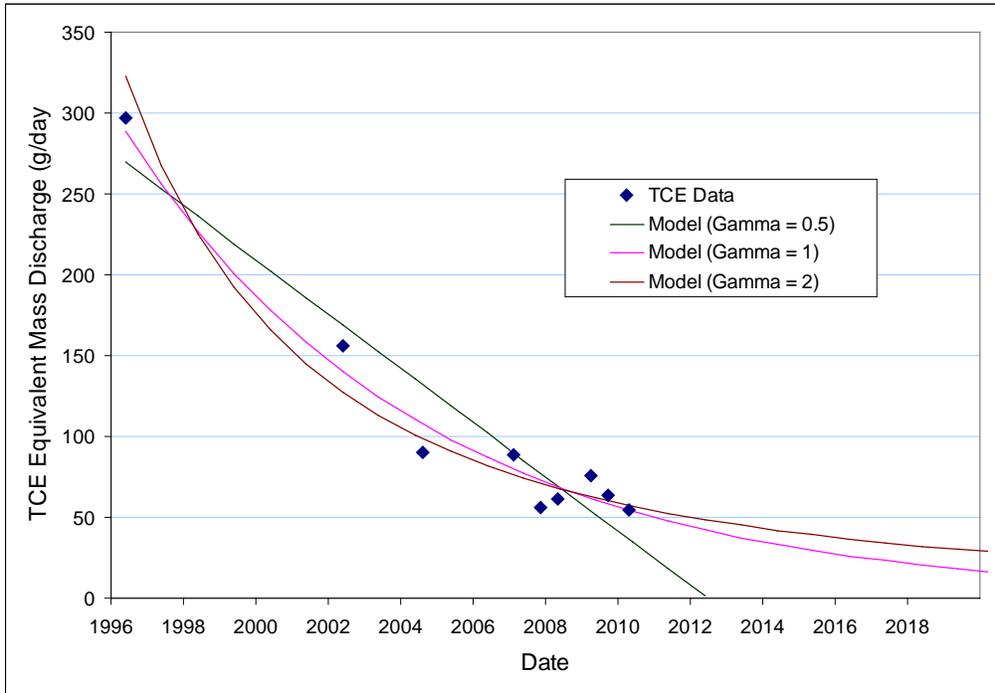Figure 8.3. Source strength functions. Measured data shown in blue diamonds, model fits shown for $\Gamma = \{0.5, 1.0, 2.0\}$ as green, purple, and brown lines.
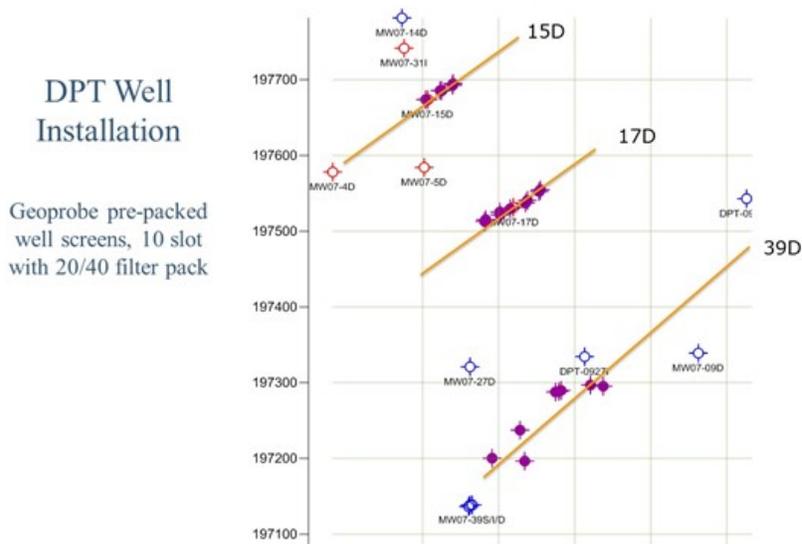

Figure 8.4. Three transects at Calf Pasture Point for PFM deployments.
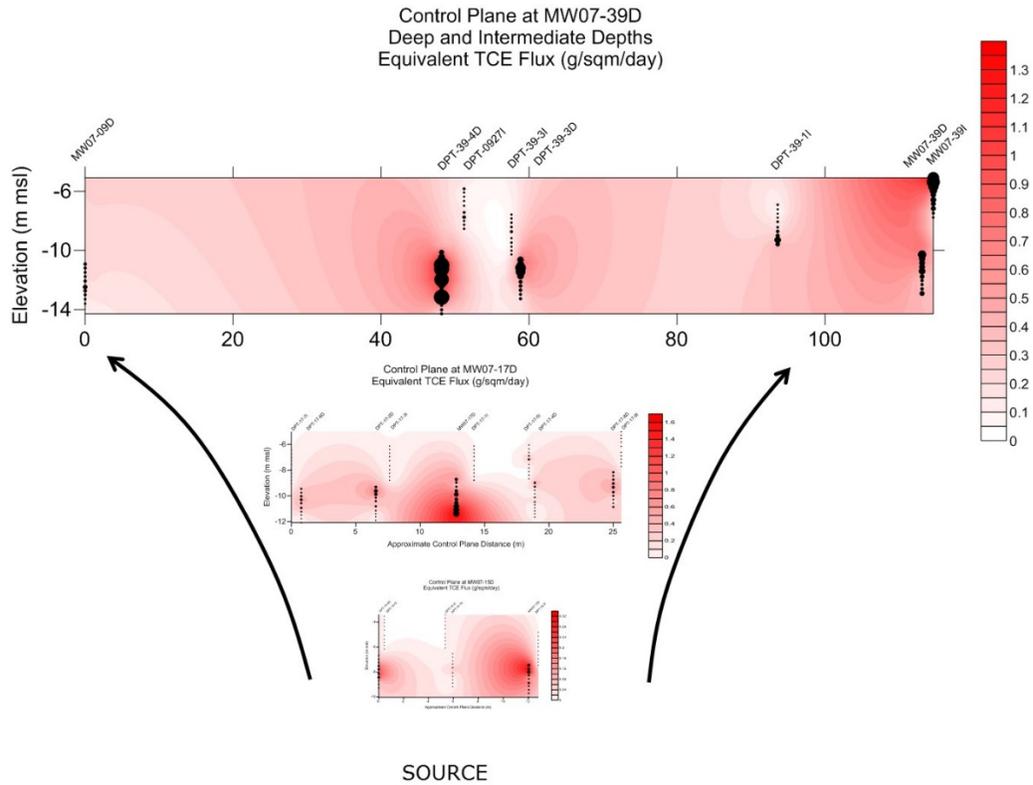
Figure 8.5.   Three transect mass flux based on PFM deployments.
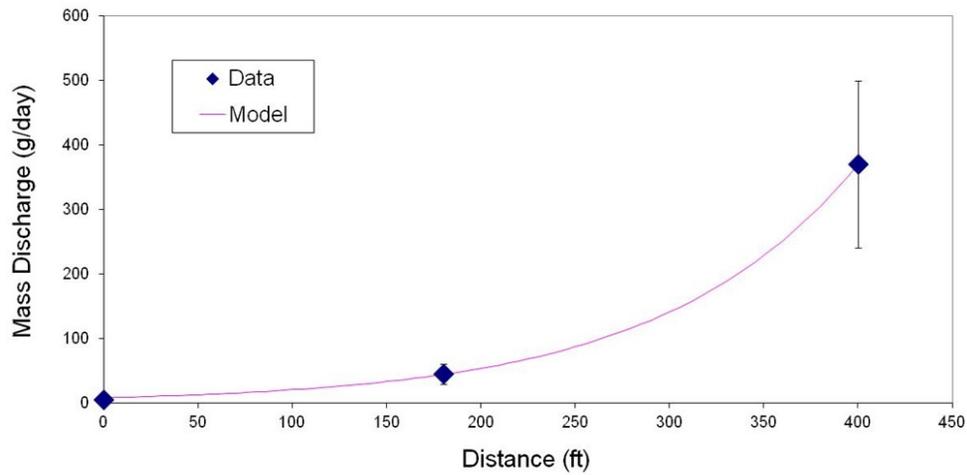

Figure 8.6. Source strength function based on three transects sampled at Calf Pasture Point.

b. Uncertainty Implications for Predicting Source Dissolution

The contaminated site is assumed to be primarily PCA with an estimated release mass of 45,000 kg. Due to the assumptions and estimate, the release mass is expected to have high uncertainty. The source strength function uses historical data and field measurements to estimate mass discharge as a function of time. The source strength function is a model of the data used to predict responses to remedial approaches, but it can contain uncertainty.

Since the limits of the source zone have not been determined, the source zone area is subject to uncertainty. Some wells were also not included in the long-term monitoring program. The wells that were selected were five wells that were about 450 feet in distance, and they had a well spacing of 90 feet. The spacing of the wells impact the accuracy of the source strength function, and uncertainty arises from the large unsampled space between the wells. The vertical distribution of the contaminants near the source zone was not evaluated, but is important for the source zone control plane. Therefore the vertical depth was assumed to equal the screened interval of the wells.

The Power-Law Model was used to predict the mass in 1968. It was assumed the model did not change with time; however, that assumption is most likely not correct, and contains uncertainty.

Plume analysis is useful to estimate mass balance between the plume and the source zone. Mass discharge from the source zone must equal the mass in the plume, as well as any degraded mass. Sorbed mass can be estimated using the site specific retardation factor, R. However, the uncertainty in the plume mass estimate also becomes a function of the uncertainty in R. Typically, plume mass estimates have a high uncertainty which is most likely from the sparse sampling density.

DNAPL source longevity can be evaluated using a first-order degradation analogy. These estimates do not include factors that may prolong contaminant mass in the source zone, such as sorption to the solid matrix and diffusion from low conductivity zones, and thus they have a high uncertainty.

Recommendations for minimizing the uncertainty in analyzing source dissolution and assessing site management decisions are provided. Wells within the source zone area that are not currently part of the long-term monitoring program should be sampled in order to better evaluate the strength and distribution of the source. It is also recommended that a preliminary passive flux meter deployment be made to evaluate the vertical distribution of the contaminants. This would also provide information to improve the source strength function. Following the passive flux meter deployment, additional soil borings are to be installed within the source zone. They will be analyzed for chlorinated ethane and ethane compounds, as well as organic carbon. After additional wells are installed, it is proposed that a second passive flux meter deployment be conducted.

10.   Back-Diffusion at Field Sites Using Flux Measurements

The former Brandywine Defense Reutilization and Marketing Office (DRMO) Yard in Brandywine, MD, is and inactive federal facility that was in operation from 1943-1987. It was

used for temporary storage of scrap materials and hazardous waste, and is now on the National Priorities List (NPL). The DRMO yard groundwater is contaminated primarily with TCE, and the plume which is underlain by the Calvert Foundation aquitard has extended past the property into a residential neighborhood. In 2006 an Interim Record of Decision (ROD) was signed, and in 2008 the ROD was implemented to capture the 3-acre core of the plume. The remaining 20-acre TCE plume was treated with In-situ Bioremediation (ISBR). 38.6 kg of VOCs were removed during 5 years of treatment.
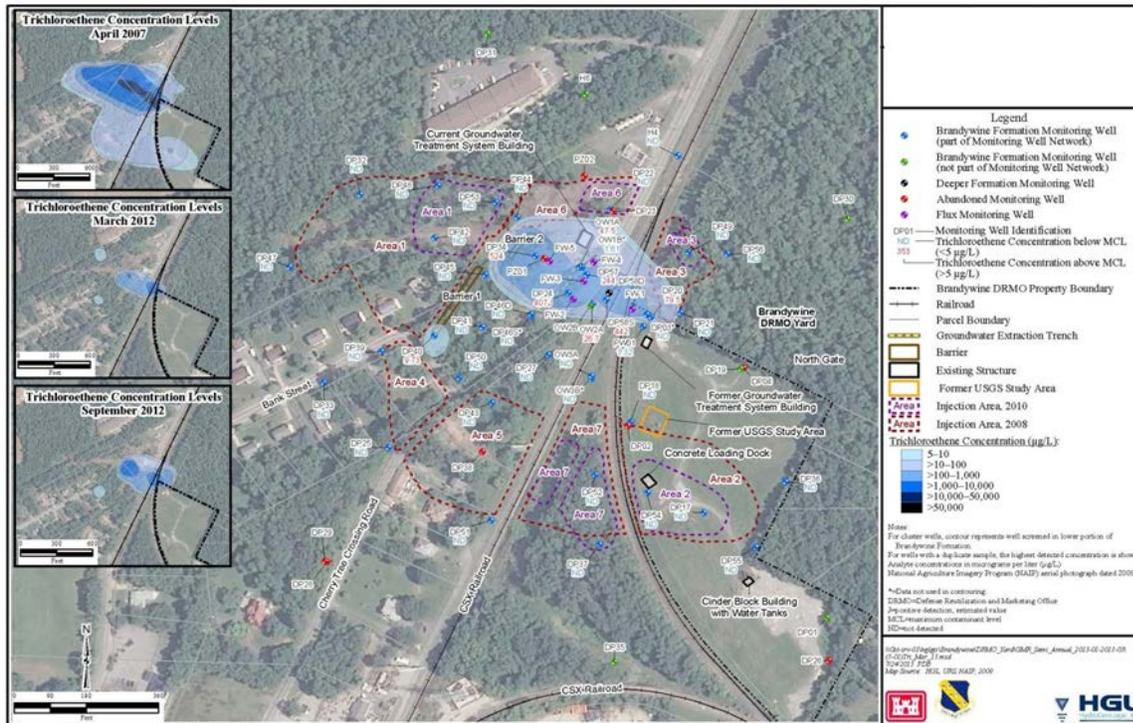

Figure 9.1: Site map showing pre-remedy extent of TCE plume (upper left), ISBR treatment areas, and post-remedy implementation TCE plume extent (March 2013).

The Brandywine Formation and the Calvert Formation are located beneath the DRMO yard. The upper Calvert is 21-30 feet below ground surface, and 30-42 feet below ground surface is the oxidize Calvert. Both are considered the aquitard. The Brandywine Formation contains the contaminant plume in the upper 12 feet, and is comprised of clay, silt, sand, and gravel. The Brandywine Formation has been determined to be heterogeneous laterally and vertically across the site, and consists of four distinct strata: Shallow Brandywine, Upper Intermediate Brandywine, Lower Intermediate Brandywine, and Deep Brandywine.

Investigation suggested that limited source material remained within the presumed release area; however a study revealed contaminant source remained when the pump and treat system were shut down. Membrane interface probe technology was selected to collect real-time, continuous data on the distribution of volatile organic compounds. The area selected for investigation was based on VOC results for soil samples. Combined with the MIP, there is a conductivity logging tool that interprets lithology. The MIP is used to identify zones of contamination. There were three electric conductivity logging tools tested: the flame ionization detector (FID), the photoionization detector (PID), and the electron capture detector (ECD). The ECD was chosen

for analysis of the site since it provides the lowest possible detection levels for chlorinated compounds.

After the MIP investigation, 5 monitoring wells with 15 foot screens were installed. Flux well (FW)-1 was installed in the presumed release area, FW-3 was installed down-gradient, FW-5 was installed further down-gradient where it was presumed contamination was not prevalent, and FW-2 and FW-4 were installed side-gradient which created a transect with FW-3. Passive Flux Meters (PFM) were deployed in each well to determine the mass flux of water and contaminant flowing per unit area in a given period of time. Three 5-foot PFMs were stacked across the entire screen length for 20 days. Once they were retrieved they were sampled at 1-foot intervals.
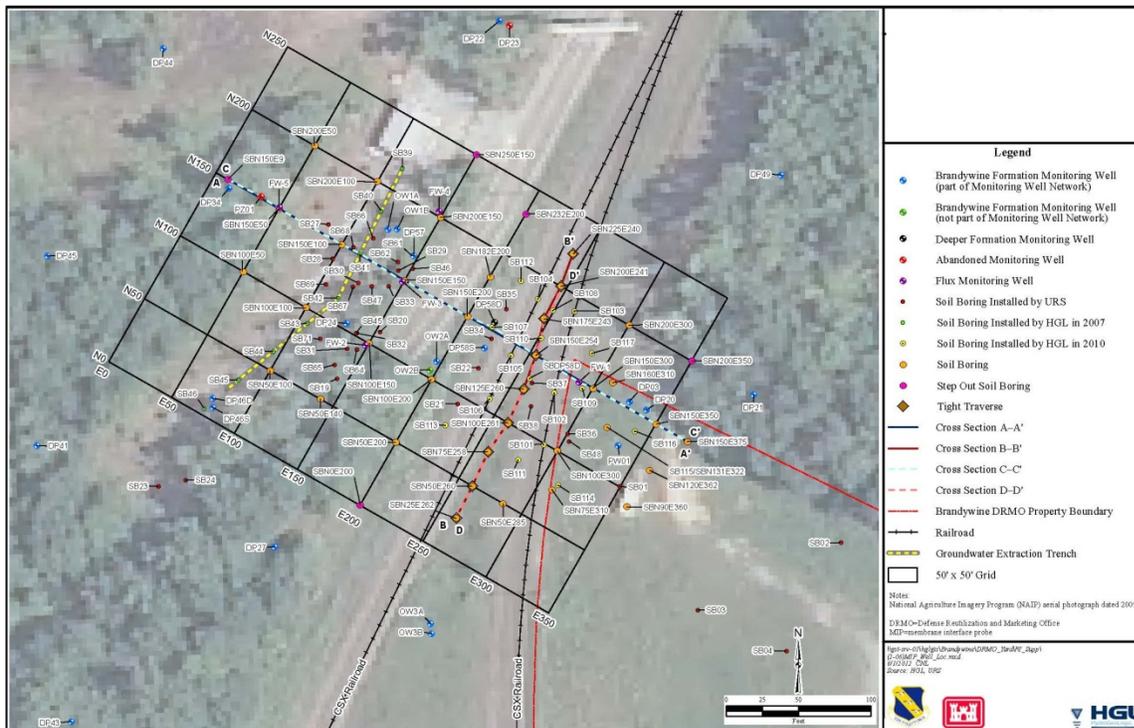
Figure 9.2: Site map showing MIP boring and flux well locations.

The ECD results indicated that the high concentrations of TCE are located in the transitional silt layer, and the highest 1 meter into the oxidized Calvert. The results also revealed that down-gradient from the release area, and west of the groundwater extraction trench, the contamination is within the groundwater, and not the transitional silt layer.
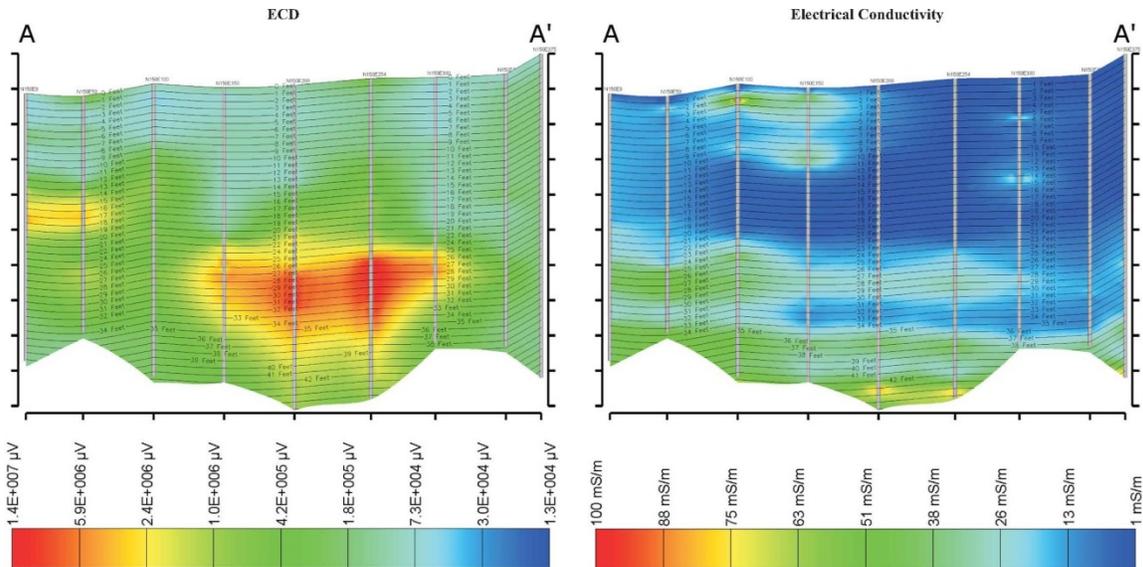
Figure 9.3: ECD and conductivity MIP responses along the axis of the plume A-A'.
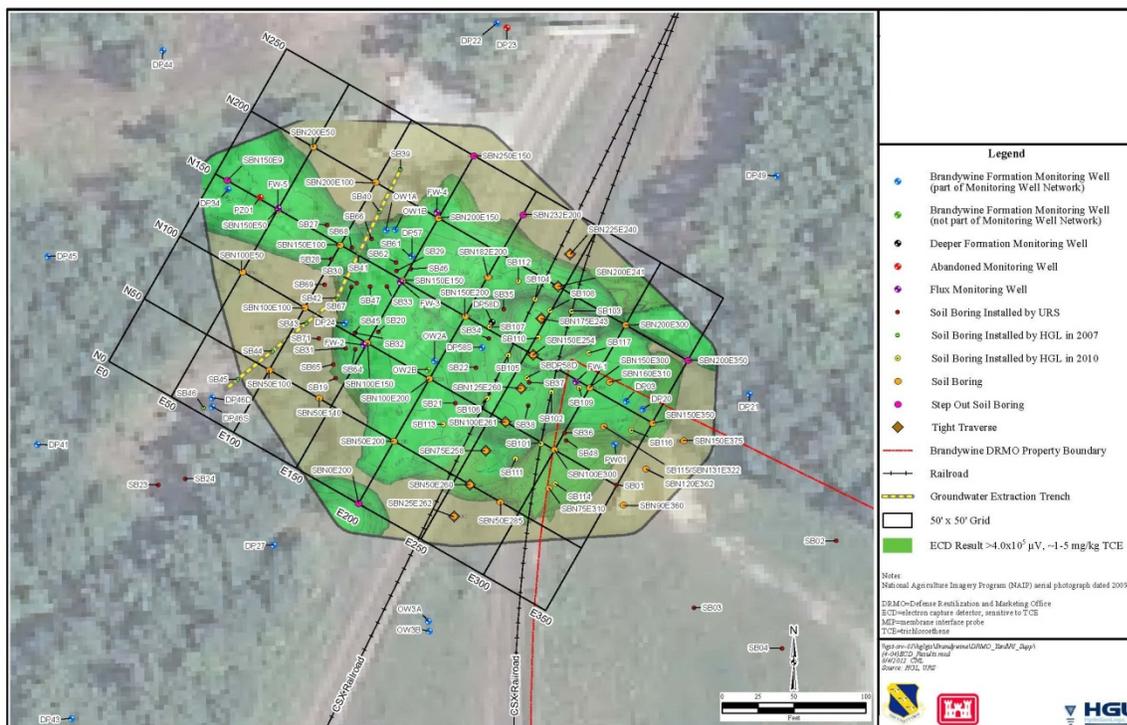
Figure 9.4: Lateral extent of TCE contamination determined by the ECD.

The TCE flux profiles, determined from the PFM results, show that the 5 wells contain significant variability and support the conceptual model of high mass flux associated with the aquitard. FW-3 contained the highest mass flux and the most significant contrast in the center of the suspected back-diffusion zone within the plume core.
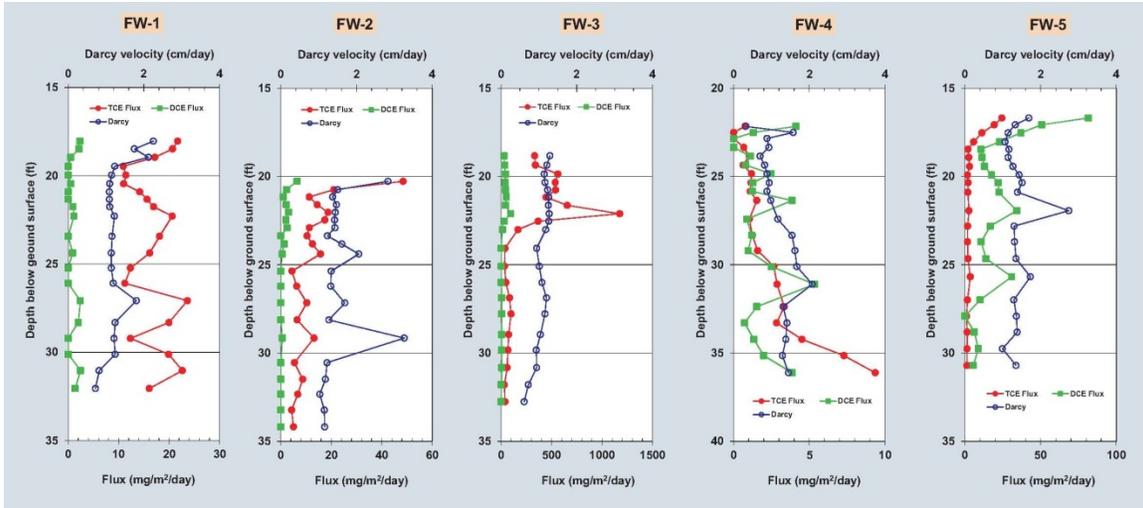
Figure 9.5: Flux well profiles showing Darcy velocity and TCE/DCE flux.

The highest mass flux was located at a depth corresponding to the transitional silt interface. The two side-gradient wells contained lower mass flux. The MIP profile for FW-2 reveals a distinct mass source 22-35 feet below ground surface that is likely providing mass flux to the Brandywine Formation. There was also a slight increase in the Darcy velocity in the flux profile that correlates with a lower conductivity response. In FW-2, the highest concentration observed was located at the upper screened portion of the well which corresponds to the top of the TCE contaminated zone. The result of this supports the conceptual model of mass diffusing from the silt interface into the Brandywine Formation.
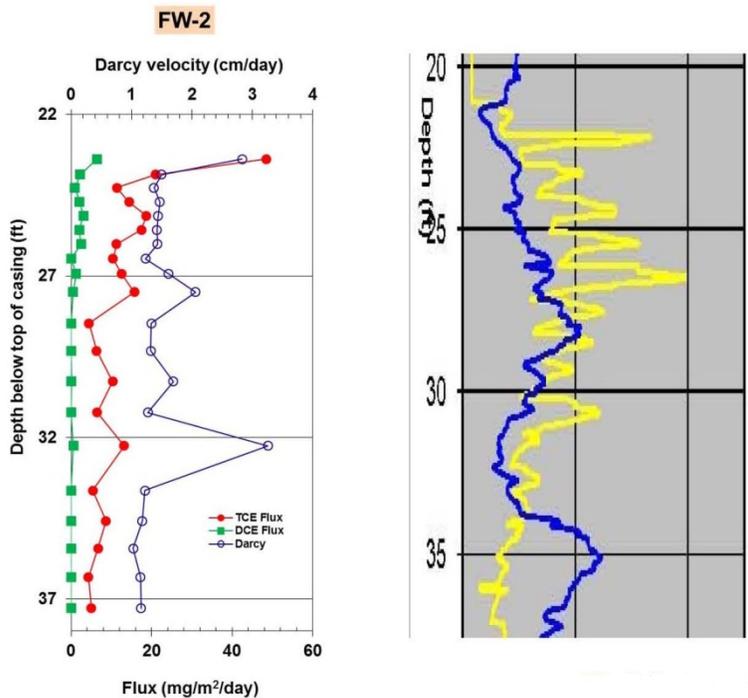
Figure 9.6: FW-2 flux profile compared to MIP ECD and conductivity responses.

FW-5 results in a much lower mass flux that FW-3, and also reveals a shift from TCE to DCE. The MIP profile shows low mass stored in the transitional silt, and suggests that mass may still be loading the aquitard.

Table 1. Mass discharge per unit width of aquifer for each well.

Well	Darcy (cm/day)	TCE (mg/m/day)	1,2-DCE (mg/m/day)
FW-1	1.3	73.8	3.8
FW-2	1.5	47.5	3.3
FW-3	1.1	891.1	71.8
FW-4	1.2	12	8.5
FW-5	1.4	15.2	79.1

The mass discharge was calculated using the summation of the product of flux and the cross-sectional flow area. The PFM based mass flux results combined with the MIP ECD profile in FW-3 provide the ability to link mass flux from back-diffusion with mass flux observed in the aquifer. A simple approach to making this link is to use a simplified one-dimensional analytical solution for back diffusion. The model is provided here and assumes a step input of constant concentration to the diffusive zone over a period of time specified as t*.

$$J_{BD}\big|_{y=0} = C_0 \sqrt{\frac{D}{\pi}} \left(\frac{1}{\sqrt{t}} - \frac{1}{\sqrt{(t-t^*)}} \right)$$

This equation provides the diffusive flux from the aquitard, J_{BD}, at some time of interest t given an estimate of the diffusion coefficient, D, and the applied loading concentration C_0. A quick estimate was made assuming a C_0 value of 100 mg/L (10% of TCE solubility) a diffusion coefficient for TCE in water (1×10^{-9} m^2/s) and a loading period t* of 20 years and 5 years after back-diffusion started (t=25 years). The calculated flux from the aquitard is 0.004 g/m^2/day. If this value is applied over a length of 50 m the mass discharge per unit width of aquifer is about 0.35 g/m/day which is of the same magnitude as observed in well FW-3 (0.89 g/m/day). This supports the back-diffusion conceptual model for the site.

The results of this study were used to characterize the nature and extent of source area contamination. The MIP results and PFM results correlate with respect to contaminant mass within the transitional silt, the locations and magnitude of diffusive mass flux, and Darcy velocity. The characteristics of the site allow the plume to persist in the Brandywine Formation, and the result of the study has provided focus on the evaluation of remedial activities and which areas to target.

11.   Conclusions and Implication for Future Research

This project focused on evaluating DNAPL source strength functions based on field data observations and the use of simple models. In this effort, several methods were proposed and evaluated as approaches that can be used to estimate parameters for DNAPL source strength functions. The results of the project have been disseminated through a series of journal articles that are listed in Appendix B. The research started with formulation of source strength functions and appropriate models and parametrization (Chen and Jawitz, 2009; Wang et al., 2013). The work then was applied to field sites with adequate data allowing determination of model parameters to characterize source strength functions for DNAPL sites (Johnston et al., 2013, 2014; Wang et al., 2014). The evaluation of uncertainty associated with determining mass discharge and source strength function was evaluated for both pumping based measurements (Xiaosong et al., 2014) and point level measurements (Brooks et al., 2015). Thus guidance in data needs and approaches were described for those interested in understating DNAPL source zone function. On a parallel effort, research was conducted to better understand the fundamentals of back diffusion from low permeability media in the subsurface. This started with a theoretical approach linking DNAPL source strength functions to back diffusion (Brown et al., 2013). Then a series of laboratory scale studies were conducted developing light transmission techniques for clays (Yang et al., 2014) and the effects of different aquifer aquitard layers (Yang et al., 2015) and finally linking to source strength functions (Yang et al., 2016). Back diffusion at field scales was then assessed (Yang et al., 2017). The project final report contains some of the material presented in these publications but also some that is currently being revised for publication such as the Calf Pasture Point study. The final report and associated journal articles will be included as part of an EPA Guidance Document of DNAPL source strength functions.

While some links between plume conditions and DNAPL source strength functions have been evaluated as part of this work, this is an area that could be greatly improved. Linking conditions in the plume to the complex behavior of DNAPL source zones is challenging given that most source zones have a history of partial remedial efforts. This complicates our understanding of the nature of the plume distribution. While Calf Pasture Point was ideal due to the lack of remedial efforts, this is the exception and better understanding of more complex source zone behavior is needed. This improved understanding of DNAPL source zone behavior and plume response can be then connected to the assimilative capacity of the aquifer and alternative mass discharge or mass flux objectives can be formulated.

Literature Cited

Annable MD, Hatfield K, Cho J, Klammler H, Parker BL, Cherry JA, Rao PSC. 2005. Field-scale evaluation of the passive flux meter for simultaneous measurement of groundwater and contaminant fluxes. Environ Sci Technol 39:7194-7201.

API (American Petroleum Institute). 2002. Estimating Mass Flux for Decision-Making: An Expert Workshop. American Petroleum Institute, Washington DC.

API (American Petroleum Institute). 2003. Groundwater Remediation Strategies Tool. Regulatory Analysis and Scientific Affairs Department. Publication 4730. American Petroleum Institute, Washington DC.

Banerjee S. 1984. Solubility of organic mixtures in water. Environ Sci Technol 18:587-591.

Basu NB, Rao PSC, Poyer IC, Annable MD, Hatfield K. 2006. Flux-based assessment at a manufacturing site contaminated with trichloroethylene. J Contam Hydrol 86:105-127.

Basu NB, Fure AD, Jawitz JW, 2008. Simplified contaminant source depletion models as analogs of multiphase simulators. J Contam Hydrol 97:87-99.

Basu NB, Rao PSC, Poyer IC, Nandy S, Mallavarapu M, Naidu R, Davis GB, Patterson BM, Annable MD, Hatfield K. 2009. Integration of traditional and innovative characterization techniques for flux-based assessment of dense non-aqueous phase liquid (DNAPL) sites. J Contam Hydrol 105:161-172.

Béland-Pelletier C, Fraser M, Barker J, Ptak T. 2011. Estimating contaminant mass discharge: a field comparison of the multilevel point measurement and the integral pumping investigation approaches and their uncertainties. J Contam Hydrol 122:63-75.

Bockelmann, A, Ptak T, Teutsch G 2001. An analytical quantification of mass fluxes and natural attenuation rate constants at a former gasworks site. J Contam Hydrol, 53, 429-453.

Bockelmann A, Zamfirescu D, Ptak T, Grathwohl P, Teutsch G. 2003. Quantification of mass fluxes and natural attenuation rates at an industrial site with a limited monitoring network: a case study. J Contam Hydrol, 60: 97-121.

Brooks, MC, Annable MD, Rao PSC, Hatfield K, Jawitz JW, Wise WR, Wood AL, Enfield CG. 2004. Controlled release, blind test of DNAPL remediation by ethanol flushing. J Contam Hydrol 69: 281-297.

Brooks, MC, Wood AL, Annable MD, Hatfield K, Cho J, Holbert C, Rao PSC, Enfield CG, Lynch K, Smith RE. 2008. Changes in contaminant mass discharge from DNAPL source mass depletion: evaluation at two field sites. J Contam Hydrol 102:140-153.

Christ JA,, Ramsburg CA, Pennell KD, Abriola LM. 2006. Estimating mass discharge from dense nonaqueous phase liquid source zones using upscaled mass transfer coefficients: An evaluation using multiphase numerical simulations, Water Resour Res 42: W11420, doi:10.1029/2006WR004886.

D'Affonseca FM, Blum P, Finkel M, Melzer R, Grathwohl P. 2008. Field scale characterization and modeling of contaminant release from a coal tar source zone. J Contam Hydrol 102:120-139.

Devlin JF, McElwee CD. 2007. Effects of measurement error on horizontal hydraulic gradient estimates. Ground Water 45: 62-73.

DiFilippo EL, Brusseau ML. 2008. Relationship between mass-flux reduction and source-zone mass removal: Analysis of field data. J Contam Hydrol 98:22–35.

Einarson MD, Mackay DM. 2001. Predicting impacts of groundwater contamination. Environ Sci Technol 35:66A-73A.

Endo, S., Schmidt, T.C. 2006. Prediction of partitioning between complex organic mixtures and water: Application of polyparameter linear free energy relationships. Environ Sci Technol 40(2), 536-545.

Enfield CG, Wood AL, Brooks MC, Annable MD, Rao PSC. 2005. Design of aquifer remediation extraction systems: (1) Describing hydraulic structure and NAPL architecture using tracers. J Contam Hydrol 81:125-147.

Falta RW. 2008. Methodology for comparing source and plume remediation alternatives. Ground Water 46:272-285.

Falta RW, Rao PSC, Basu N. 2005a. Assessing the impacts of partial mass depletion in DNAPL source zones: I. Analytical modeling of source strength functions and plume response. J Contam Hydrol 78: 259-280.

Falta RW, Basu N, Rao PSC. 2005b. Assessing the impacts of partial mass depletion in DNAPL source zones: II. Coupling source strength functions to plume evolution. J Contam Hydrol 79:45-66.

Fraser M, Barker JF, Butler B, Blaine F, Joseph S, Cooke C. 2008. Natural attenuation of a plume from an emplaced coal tar creosote source over 14 years. J Contam Hydrol 100:101–115.

Fure AD, Jawitz JW, Annable MD. 2006. DNAPL source depletion: linking architecture and flux response. J Contam Hydrol 85:118-140.

Goltz MN, Huang J, Close ME, Flintoft MJ, Pang L. 2008. Use of tandem circulation wells to measure hydraulic conductivity without groundwater extraction. J Contam Hydrol 100:127-136.

Goltz MN., Close ME, Yoon H, Huang J, Flintoft MJ, Kim S, Enfield C. 2009. Validation of two innovative methods to measure contaminant mass flux in groundwater, J Contam Hydrol 106:51-61.

Guilbeault MA, Parker BL, Cherry JA. 2005. Mass and flux distributions from DNAPL zones in sandy aquifers. Ground Water 43: 70-86.

Hatfield K, Rao PSC, Annable MD, Campbell T. 2002. Device and method for measuring fluid and solute fluxes in flow systems, Patent US 6,402,547 B1. U.S. Patent Office, Washington DC, USA.

Hatfield, K, Annable, MD, Cho J, Rao PSC, Klammler H. 2004. A direct passive method for measuring water and contaminant fluxes in porous media. J Contam Hydrol 75:155-181.

Henderson JK, Falta RW, Freedman DL. 2009. Simulation of the effect of remediation on EDB and 1,2-DCA plumes at sites contaminated by leaded gasoline, J Contam Hydrol 108(1-2), 29-45.

Illangasekare TH, Ramsey J, Jensen KH, Butts BM. 1995. Experimental study of movement and distribution of dense organic contaminants in heterogeneous aquifers. J Contam Hydrol 20:1-25.

ITRC (Interstate Technology & Regulatory Council). 2003. Assessing the performance of DNAPL source reduction remedies. Dense Nonaqueous Phase Liquids Team, Washington, DC, USA.

ITRC. 2010. Use and measurement of mass flux and mass discharge. MASSFLUX-1. Integrated DNAPL Site Strategy Team, Washington, DC, USA.

Jawitz, JW, Annable MD, Demmy GG, Rao PSC. 2003. Estimating non-aqueous phase liquid spatial variability using partitioning tracer higher temporal moments. Water Resour Res 39:1192. doi;10.1029/2002WR001309.

Jawitz JW, Fure AD, Demmy GG, Berglund S, Rao PSC. 2005. Groundwater contaminant flux reduction resulting from nonaqueous phase liquid mass reduction. Water Resour Res 41: W10408.

Kavanaugh MC, Rao PSC, eds. 2003. The DNAPL Remediation Challenge: Is There a Case for Source Depletion? EPA/600/R-03/143. National Risk Management Research Laboratory, Office of Research and Development, U.S. Environmental Protection Agency, Cincinnati, OH, USA.

King, MWG, Barker JF. 1999. Migration and natural fate of a coal tar creosote plume 1. Overview and plume development. J Contam Hydrol 39:249-279.

King MWG, Barker JF, Devlin JF, Butler BJ. 1999. Migration and natural fate of a coal tar creosote plume 2. Mass balance and biodegradation indicators. J Contam Hydrol 39:281-307.

Klammler H, Hatfield K, Annable MD. 2007a. Concepts for measuring horizontal groundwater flow directions using the passive flux meter. Adv Water Resour 30:984-997.

Klammler H, Hatfield K, Annable MD, Agyei E, Parker BL, Cherry JA, Rao PSC. 2007b. General analytical treatment of the flow field relevant to the interpretation of passive fluxmeter measurements, Water Resour Res 43: W04407. doi:10.1029/2005WR004718.

Klammler H, Hatfield K, Luz JAG, Annable MD, Newman M, Cho J, Peacock A, Stucker V, Ranville J, Cabaniss S, Rao PS. 2012. Contaminant discharge and uncertainty estimates from passive flux meter measurements, Water Resour Res 48: W02512, doi:10.1029/2011WR010535.

Kram ML, Keller AA, Rossabi J, Everett LG. 2002. DNAPL characterization methods and approaches, part 2: Cost comparison. Ground Water Monit Remed 22:46-61.

Kübert M Finkel M 2006. Contaminant mass discharge estimation in groundwater based on multi-level point measurements: a numerical evaluation of expected errors. J Contam Hydrol 84:55-80.

Kueper BH, Redman D, Starr RC, Reitsma S, Mah M 1993. A field experiment to study the behavior of tetrachloroethylene below the water table: Spatial distribution of residual and pooled DNAPL. Ground Water 31:756–766.

Lane WF, Loehr RC 1992. Estimating the equilibrium aqueous concentrations of polynuclear aromatic hydrocarbons in complex mixtures. Environ Sci Technol 26:983-990.

Lee LS, Rao PSC, Okuda I. 1992. Equilibrium partitioning of polycyclic aromatic hydrocarbons from coal tar into water, Environ Sci Technol 26:2110-2115.

Lemke LD, Abriola LM, Lang JR. 2004. Influence of hydraulic property correlation on predicted dense nonaqueous phase liquid source zone architecture, mass recovery and contaminant flux. Water Resour Res 40:W12417.

Li KB, Goovaerts P, Abriola LM. 2007. A geostatistical approach for quantification of contaminant mass discharge uncertainty using multilevel sampler measurements. Water Resour Res 43: W06436.

Mahjoub, B., Jayr, E., Bayard, R., Gourdon, R. 2000. Phase partition of organic pollutants between coal tar and water under variable experimental conditions. Water Research 34(14): 3551-3560.

NRC (National Research Council). 2004. Contaminants in the Subsurface: Source Zone Assessment and Remediation. The National Academies Press, Washington DC, USA.

Parker JC, Park E. 2004. Modeling field-scale dense nonaqueous phase liquid dissolution kinetics in heterogeneous aquifers. Water Resour Res 40: W05109. doi; 10.1029/2003WR002807.

Parker BL, Chapman SW, Guilbeault MA 2008. Plume persistence caused by back diffusion from thin clay layers in a sand aquifer following TCE source-zone hydraulic isolation, J Contam Hydrol 102:86-104.

Ptak T, Schirmer M, Teutsch G. 2000. Development and performance of a new multilevel groundwater sampling system. In Wickramanayake GB, Gavaskar AR, Kelley ME, Nehring KW, eds, Risk, Regulatory and Monitoring Considerations: Remediation of Chlorinated and Recalcitrant Compounds. Battelle Press, Columbus, OH, USA, pp 95-102.

Rao PSC, Jawitz JW. 2003. Comment on "Steady state mass transfer from single-component dense nonaqueous phase liquids in uniform flow fields" by Sale TC, McWhorter DB. Water Resour Res 39: 1068.

Rao, PSC, Jawitz J, Enfield C, Falta R, Annable M, Wood A. 2002. Technology integration for contaminated site remediation: Cleanup goals and performance criteria. In Groundwater Quality 2001. Proceedings, Thornton S Oswald S, eds. IAHS Publication 275. pp 571-578.

Rein A, Bauer S, Dietrich P, Beyer C. 2009. Influence of temporally variable groundwater flow conditions on point measurements and contaminant mass flux estimations, J Contam Hydrol 108:118-133.

Sale TC, McWhorter DB. 2001. Steady-state mass transfer from single-component dense non-aqueous phase liquids in uniform flow fields. Water Resour Res 37:393-404.

Schwede RL, Cirpka OA 2009. Use of steady-state concentration measurements in geostatistical inversion. Adv Water Resour 32:607-619.

Soga K, Page JWE, Illangasekare TH. 2004. A review of NAPL source zone remediation efficiency and the mass flux approach. J Hazard Mater 110:13-27.

Stroo HF, Unger M, Ward CH, Kavanaugh MC, Vogel C, Leeson A, Marqusee JA, Smith BP. 2003. Remediating chlorinated solvent source zones. Environ Sci Technol 37:224A-230A.

Teutsch, G, Ptak, T, Schwarz R, Holder T. 2000. Ein neus integrales Verfahren zur Quantifizierung der Grundwasserinnission: I. Theoretische Grundlagen. Grundwasser 4:170-175.

Thomson NR, Fraser MJ, Lamarche C, Barker JF, Forsey SP 2008. Rebound of a coal tar creosote plume following partial source zone treatment with permanganate. J Contam Hydrol 102:154-171.

Wang, F., M.D. Annable, C.F. Schaefer, T.D. Ault, J. Cho and J.W. Jawitz. Enhanced Aqueous Dissolution of a DNAPL Source to Characterize the Source Strength Function. Journal of Contaminant Hydrology 169, 75–89, 2014.

Wood, AL, Enfield CG, Annable MD, Brooks MC, Rao PSC, Sabatini D, Knox R. 2005. Design of aquifer remediation extraction systems: (2) Estimating site-specific performance and benefits of partial source removal. J Contam Hydrol 81:148-166.

Zhu J, Sykes JF. 2004. Simple screening models of NAPL dissolution in the subsurface, J Contam Hydrol 72:245–258.

Appendix A: Supporting Data

Table A1. Summary of mass discharge measurements (g/day) using Method 1 at Calf Pasture Point.

Control Plane	Method 1		
	PFM3	PFM4	PFM4 Subset
15I	0.1	0.0	-
15D	5.4	6.3	-
15 Sum	5.5	6.3	-
17I	2	1	-
17D	35	36	-
17 Sum	37	37	-
39S	72	101	71
39I	68	164	66
39D	254	247	311
39 Sum	394	512	448

Table A2. Summary of mass discharge measurements (g/day) using Methods 2a and 2b.

Control Plane	Method 2a			Method 2b		
	PFM3	PFM4	PFM4 Subset	PFM3	PFM4	PFM4 Subset
15I	0.0	0.0	-	0.0	0.0	-
15D	5.4	6.2	-	4.9	4.7	-
15 Sum	5.5	6.2	-	4.9	4.7	-
17I	1.9	1.3	-	1.7	0.8	-

	PFM3	PFM4		PFM3	PFM4	
17D	35	36	-	35	36	-
17 Sum	37	37	-	37	37	-
39S	72	100	71	68	58	36
39I	64	159	63	63	101	15
39D	239	227	289	244	177	233
39 Sum	375	486	423	375	336	284

Table A3. Summary of mass discharge measurements (g/day) using Method 3.

Control Plane	Method 3		
	PFM3	PFM4	PFM4 Subset
15I	0.1	0.0	-
15D	5.3	6.8	-
15 Sum	5.4	6.8	-
17I	2.0	0.8	-
17D	36	36	-
17 Sum	38	37	-
39S	71	79	49

Summary of Mass Discharges for PFM3 and PFM4												
Control Plane	Actual Well Spacing[1]			Fitted Straight Control Plane						Curvilinear Control Plane[4]		
				Nearest Point[2]			Streamline[3]					
	PFM3	PFM4	PFM Sub[5]	PFM3	PFM4	PFM4 Sub[5]	PFM3	PFM4	PFM4 Sub[5]	PFM3	PFM4	PFM4 Sub[5]
15I	0	0		0	0		0	0		0	0	
15D	5	6		5	6		5	5		5	7	
17I	2	1		2	1		2	1		2	1	
17D	35	36		35	36		35	36		36	36	
39S	72	101	71	72	100	71	68	58	36	71	79	49
39I	68	164	66	64	159	63	63	101	15	86	143	19
39D	254	247	311	239	227	289	244	177	233	265	285	252
15I,D	6	6		6	6		5	5		5	7	
17I,D	37	37		37	37		36	36		38	37	
39s,I,d	395	513	448	375	485	423	375	337	284	421	507	320

Appendix B: List of Journal Publications

Yang M., M.D. Annable, J.W. Jawitz. Forward and back diffusion through argillaceous formations. In press, Water Resources Research.

Yang M., M.D. Annable, J.W. Jawitz. Field-scale forward and back diffusion through low-permeability zones. In press, to Journal of Contaminant Hydrology.

Yang, M., Annable, M.D., J.W Jawitz. Solute source depletion control of forward and back diffusion through low-permeability zones, Journal of Contaminant Hydrology, 193, 54-62, 2016.

Brooks, M.C., K.Y. Cha, A.L. Wood and M.D. Annable. Screening-Level Estimates of Mass Discharge Uncertainty from Point Measurement Methods. Journal of Contaminant Hydrology, 177 (167-182), 2015.

Yang, M., Annable, M.D., Jawitz, J.W. Back diffusion from thin low permeability zones. Environ. Sci. Technol. 49, 415−422, 2015.

Xiaosong Chen, X.M.C. Brooks, A.L. Wood. The uncertainty of mass discharge measurements using pumping methods under simplified conditions. Journal of Contaminant Hydrology, 156 (2014) 16–26.

Wang, F., M.D. Annable, C.F. Schaefer, T.D. Ault, J. Cho and J.W. Jawitz. Enhanced Aqueous Dissolution of a DNAPL Source to Characterize the Source Strength Function. Journal of Contaminant Hydrology 169, 75–89, 2014.

Johnston, C.D., G.B. Davis, T.P. Bastow, R.J. Woodbury, P.S.C. Rao, M.D. Annable, S. Rhodes. Mass Discharge Assessment at a Brominated DNAPL Site: Effects of known DNAPL source mass removal. Journal of Contaminant Hydrology, 164 (100-113), 2014.

Yang, M., J.W. Jawitz, M.D. Annable. Light reflection visualization to determine solute diffusion into clays. Journal of Contaminant Hydrology, 161(1-9), 2014.

Wang, F., M.D. Annable, J.W. Jawitz. Field-scale Prediction of Enhanced DNAPL Dissolution Based on Partitioning Tracers, Journal of Contaminant Hydrology, 152(147-158), 2013.

Johnston C.D., G.B. Davis, T.P. Bastow, M.D. Annable, M.G. Trefry, A. Furness, Y. Geste, R.J. Woodbury, P.S.C. Rao, and S. Rhodes. The Use of Mass Depletion–Mass Flux Reduction Relationships During Pumping to Determine Source Zone Mass of a Reactive Brominated-Solvent DNAPL. Journal of Contaminant Hydrology, 144, 122–137, 2013.

Brown G.B., M.C. Brooks, A.L. Wood, M.D. Annable, J. Huang. 2013. Aquitard contaminant storage and flux resulting from dense nonaqueous phase liquid source zone dissolution and remediation. Water Resources Research, 48(W06531), DOI: 10.1029/2011WR011141.

Chen, X., and Jawitz, J.W., 2009. Convergence of DNAPL source strength functions with site age. Environmental Science & Technology, 43(24): 9374-9379.